

PAVEMENT ANALYSIS AND DESIGN SOFTWARE (PADS) BASED ON THE SOUTH AFRICAN MECHANISTIC-EMPIRICAL DESIGN METHOD

H L Theyse and M Muthen

Transportek CSIR, P O Box 395, Pretoria, 0001

INTRODUCTION

The TRH4 Structural Design of Flexible Pavements for Inter-urban and Rural Roads guideline document (1) was revised during the period 1994 to 1995. One of the major changes to the document was the introduction of an approximate design reliability associated with each of the four road categories listed in Table 1.

Table 1: Road categories and approximate design reliability

Road Category	Description	Approximate design reliability (%)
A	Interurban freeways and major interurban roads	95
B	Interurban collectors and major rural roads	90
C	Rural roads	80
D	Lightly trafficked rural roads	50

This specification of the approximate design reliability for each road category had its biggest impact on the pavement design catalogue contained in the TRH4 document. Firstly, the catalogue had to be expanded to include suggested designs for road category D and secondly, the design method used to develop the designs for all four road categories had to incorporate design reliability in some way.

TRH4 recommends that the final selection of a particular pavement design is based on the life-cycle cost comparison of a number of alternative designs. The purpose of the design method, and the pavement catalogue in TRH4 which is just an application of the design method, is therefore not the selection of the final design but to provide the designer with a number of design alternatives for the particular bearing capacity for which he is designing. Although the design method is not the final selection tool it must still provide an unbiased estimate of the bearing capacity of each design regardless of the pavement type to ensure that all designs are treated on an equal basis in the cost analysis. If the bearing capacity of a particular type of pavement is overestimated, it will have an unfair advantage in the cost analysis component of the design process.

The desired design method for the revision of the TRH4 pavement design catalogue therefore had to adhere to the following requirements:

- Although not intended as a pavement behaviour and performance simulation tool it had to provide a reasonably accurate estimate of the bearing capacity of a pavement structure.
- Design models for a variety of pavement material types had to be included in the design method.
- Unbiased design bearing capacity estimates had to be made regardless of pavement type.
- Different levels of approximate design reliability had to be provided for in a scientific way not merely based on subjective assessment.
- The rules of the design models had to be applied consistently to all pavement type, road category and design bearing capacity combinations.

The South African Mechanistic-Empirical Design Method (SAMDM) had the potential to satisfy the above requirements but did not include design reliability. Approximate design reliability, related to the design reliability of the four road categories was therefore introduced in all the distress models contained in the SAMDM as a first step of development. A spreadsheet macro program was then developed as a second step because of the number of pavement designs which had to be evaluated for the design catalogue. This macro program was, however, limited in its application as it was not a standalone software package. It was therefore decided to develop a commercial software package based on the SAMDM.

This paper discusses the following topics:

1. Variability and reliability in mechanistic-empirical pavement design and the introduction of approximate design reliability in the SAMDM.
2. The content of and procedure followed by the SAMDM.
3. The Pavement Analysis and Design Software (PADS) package.

VARIABILITY AND RELIABILITY IN PAVEMENT DESIGN

The development of mechanistic-empirical design methods historically aimed at developing more accurate pavement models with a lot of emphasis on developing the deterministic or mechanistic part of the model. The deterministic model used in these design methods evolved from multi-layer, linear-elastic solution schemes using integral transformation techniques for solving the stress and strain response of the pavement system to loading to the point where complex finite element solution schemes are now used, albeit mostly for research work and not routine design. There has, however, recently been an increased awareness of the inherent empirical component and associated variability of these design methods. Several techniques have as a result been developed to accommodate variability in the design process. One must, however, critically investigate these techniques to understand their real impact on the design process. The general concepts of what one would like to achieve by introducing variability and design reliability are therefore discussed firstly, followed by a discussion on how to introduce these concepts in the design process.

Variability and Design Reliability

As mentioned previously the historical intention of mechanistic-empirical design was for the design process to be largely deterministic. Although it will never be possible to have a totally deterministic model, let's assume that Figure 1(a) represents the output from such a model for predicting the bearing capacity of a pavement.

Because of the real variation in the geometry, material properties and material response of the physical road, the true response of the bearing capacity of the pavement will have a distribution with a true mean. The output from the deterministic model will, however, only be a single predicted value. The accuracy of the model will determine how far the predicted value lies from the true mean of the real bearing capacity distribution.

Figure 1(b) illustrates the output from a probabilistic pavement design method consisting of a distribution of values for the pavement bearing capacity of which the mean is an estimate of the true pavement bearing capacity. The width of the generated distribution of pavement bearing capacity represents the precision of the model and should attempt to estimate the true variation in pavement bearing capacity.

It is possible to make a number of statements regarding the real impact of using a probabilistic approach from the concepts displayed in Figure 1:

- The accuracy of the pavement design process is not necessarily increased by using a probabilistic method. The same basic computational algorithms are normally used in probabilistic models as those used in conventional mechanistic-empirical design methods and therefore the accuracy of the probabilistic method should be exactly the same as the accuracy of conventional design methods.
- The variation in the distribution of pavement bearing capacity values generated by the probabilistic model does not necessarily reflect the true variation in the pavement bearing capacity of the physical system. Ideally the precision of the model should be the same as the variation of the true distribution of pavement bearing capacity for the model to reflect true pavement response.
- The ultimate pavement design model should generate a distribution of pavement bearing capacity values of which the **mean and variation** do not differ significantly from the true mean and true variation of the bearing capacity distribution of the real system. Design reliability is meaningless unless this principle is adhered to. Continued effort on improving both the accuracy and precision of the model is therefore required. An argument often used by the proponents of the probabilistic method is that the variation in the real system and model is in any case so big that it masks the accuracy of the model and that improvement of the accuracy of the model should not really receive a lot of attention. This statement holds if the offset between the true and modelled means are small relative to the variation in the results but not if there are large deviations from the true mean. This point is, however, difficult to quantify and substantiate as the true distribution is very seldom known.

Methods for Incorporating Variation and Reliability in Pavement Design

Figure 2 shows a simplified diagrammatic representation of a mechanistic-empirical design procedure. The two highlighted blocks of the diagram represents the components of the process where measured data are input. Every single input parameter that is measured empirically and entered into the system, has a certain variation associated with it because of the natural variability of the parameter and error in the measurement technique which is hopefully small. Assuming that the variation in the model is a true reflection of the actual variation of the physical system, there are therefore two entry points for introducing variability in the design process namely in the input data which characterize the system and in the performance models which model the distress or deterioration of the system in response to loading.

The possible sources of variation in the model are therefore:

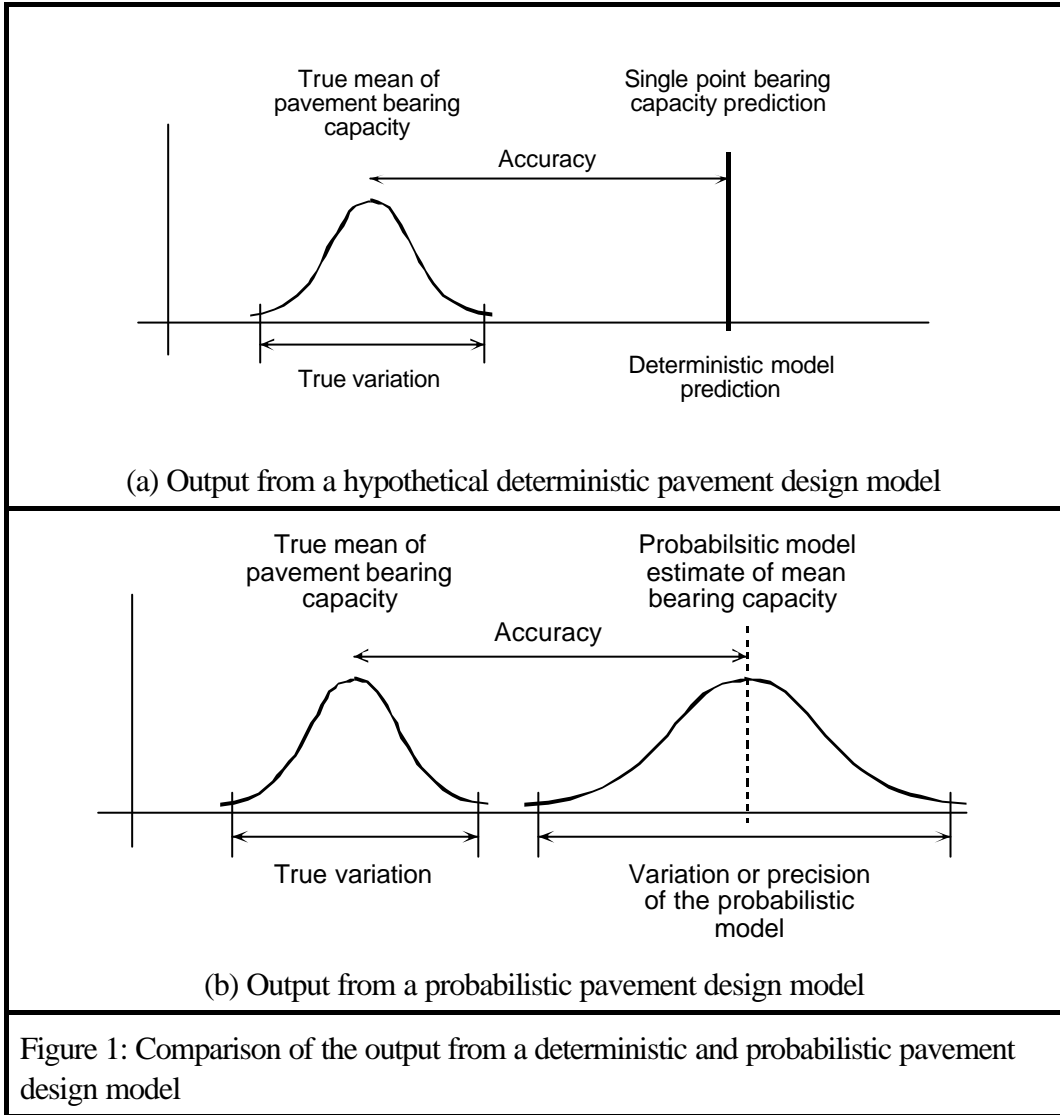
System geometry input	Layer thickness variation
Material input parameters	Variation in stiffness and Poisson's ratio
	Variation in material strength parameters (this may actually be regarded as part of the performance model)

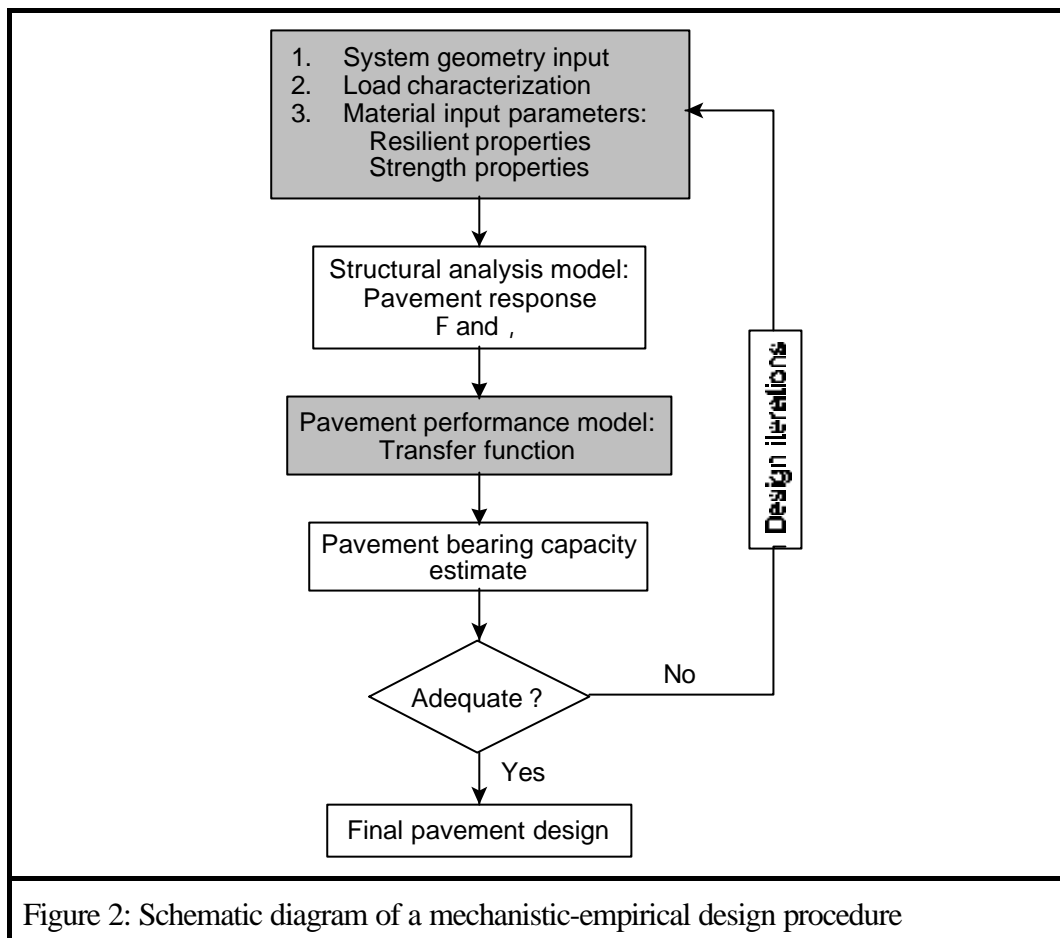
Load characterization

Variation in contact stress magnitude (influenced by dynamic effects, vehicle loading and tyre inflation pressures)

Traffic wander

Pavement performance models Natural variation in the distress response of a single material type subjected a single stress condition.





Different techniques are, however, required for incorporating the variation in the input parameters and the variation in material performance response in the design process.

Techniques for incorporating the variation of the input parameters

There are two generally accepted techniques for accommodating the variation of the input parameters in the design model. These are the Monte-Carlo (2) and Rosenblueth (3) techniques.

The Monte-Carlo simulation technique randomly generates huge numbers of input data sets from the known distributions of the input parameters while adhering to the distribution characteristics of the individual input parameters. These input data sets serve as input to the structural analysis model and by running the structural analysis model successively using the different input data sets, a distribution of the resilient pavement response parameters is generated. The distribution of the pavement response parameter in turn serves as the input to the pavement performance model.

The Rosenblueth technique is actually a point estimate approximation technique whereby the continuous distribution of a particular input parameter is approximated by a discrete distribution of two adequately chosen values of that input parameter. The criteria for selecting the two discrete values are that the first three statistical moments of the continuous and discrete distributions must be equal. Amongst others, Van Cauwelaert (4) suggested to increase the number of discrete points to three with the third point equal to the mean of the continuous distribution which then requires an additional condition that the fourth statistical moment of both distributions must be equal. The detail of selecting the values of the input parameters for the discrete

distributions is not crucial to this discussion and the reader is referred to Eckmann (3). What is of importance is that instead of randomly generating a multitude of input data sets for which structural analyses are done, only combinations of the discrete input values are analysed.

Incorporation of the variation in material distress response in the design process

The pavement performance models or transfer functions are normally obtained from the regression analysis of a set of performance data for a particular material type and distress mode as illustrated in Figure 3.

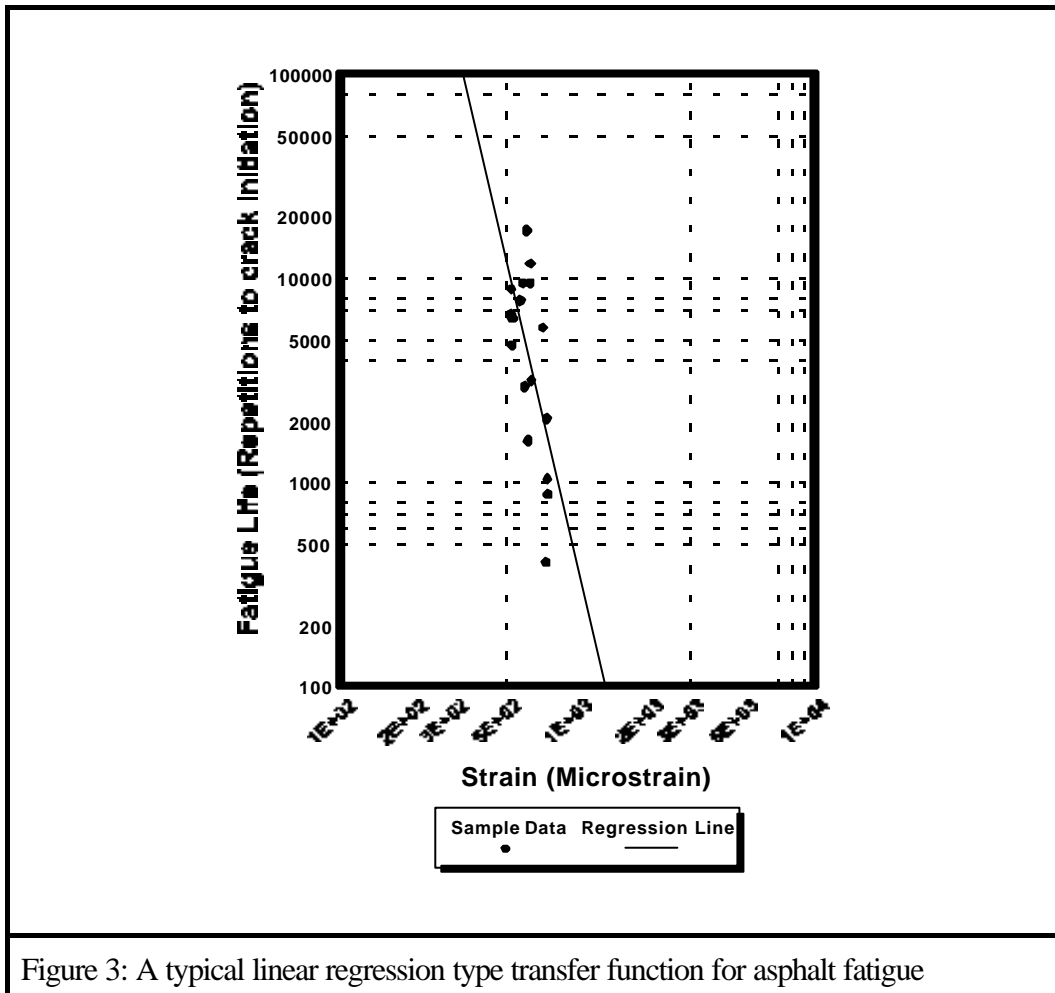


Figure 3: A typical linear regression type transfer function for asphalt fatigue

The variation in fatigue response at a single value of the pavement response parameter (which is the strain at the bottom of the asphalt layer in this particular example) is quite evident from the data in Figure 3. This source of variation is rarely incorporated in pavement design whereas the incorporation of the variation in the value of the input parameters has been investigated by a number of researchers of which examples have been quoted in the preceding section. Jooste (2) hinted at this source of variation but did not include it in his modelling.

The way to incorporate the variation of the distress response in the design procedure is to make use of statistical probability limits. Figure 4 illustrates the difference between three possible types of statistical limits applicable to regression analysis.

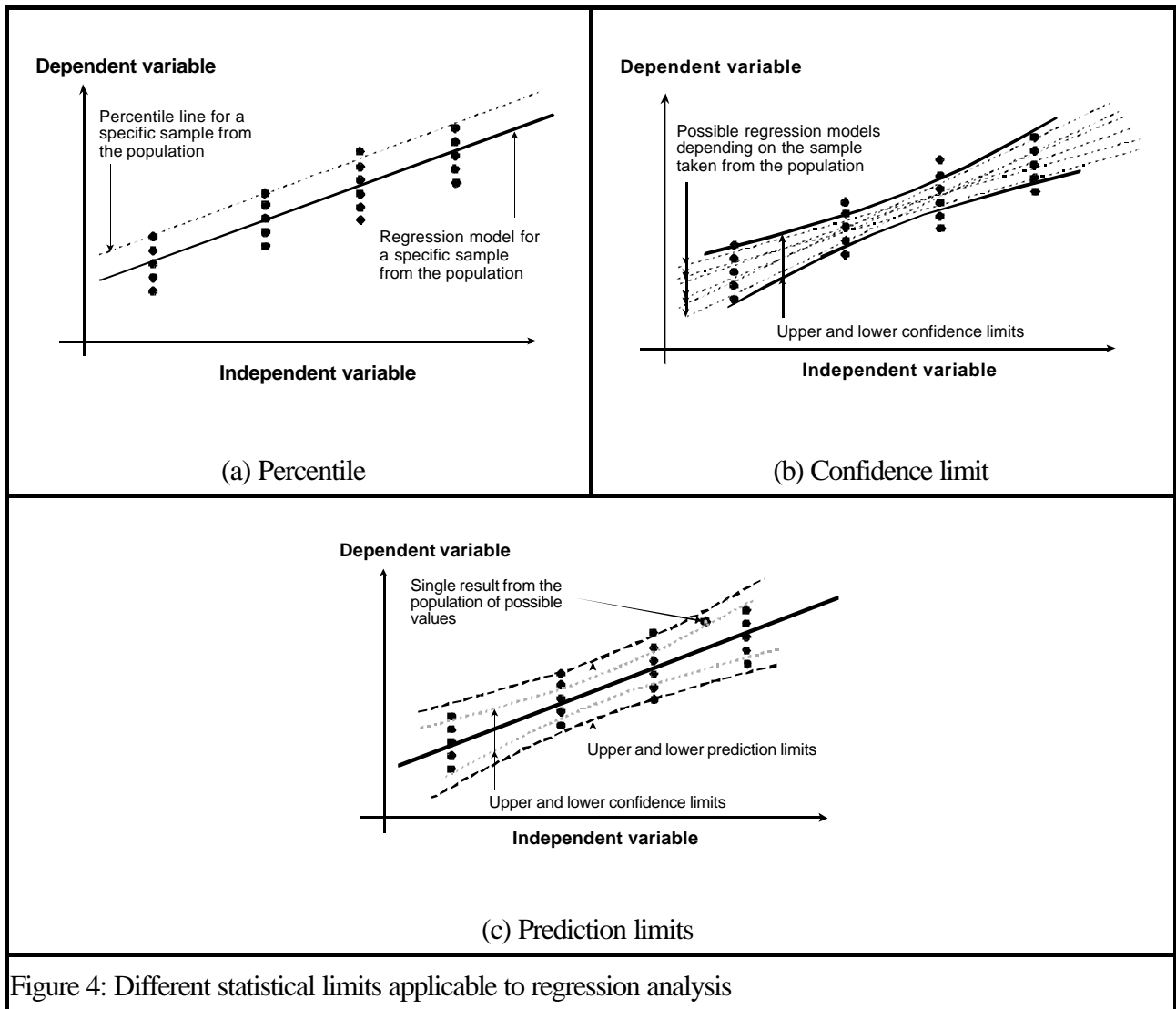


Figure 4: Different statistical limits applicable to regression analysis

Figure 4(a) shows an hypothetical example of a percentile line at a constant offset from the regression line for a specific sample taken from the population of possible values. The regression model and percentile line are only valid for this specific sample and do not provide any information on the population from which the sample was taken. The percentile line indicates the boundary below which a certain percentage of the observations from the sample lies. The amount by which the percentile line is offset from the regression model is determined by the distribution of the residuals (difference between the observed and modelled values) around the regression model.

Figure 4(b) shows a number of different regression models for different samples taken from the same population with an hypothetical set of confidence limits indicating the boundaries within which the true regression model for the population will lie with a certain probability. The confidence limits therefore delineate the area within which the position of the regression model may lie but do not give any information on the spread of the data in the population.

Figure 4(c) shows a data sample with the regression model, confidence and prediction limits for the particular sample. The prediction limits indicate the boundaries within which a certain percentage of the individual data points from the population will lie. The prediction limits therefore delineate the area within which the individual data points from any sample taken from the population will lie with a certain probability. The prediction limits for a specific sample lie further away from the regression model than the confidence limits for the same sample.

The lower prediction limit is therefore the appropriate statistical limit to be used for design where the designer's aim is to ensure that if the actual bearing capacity of the designed facility is sampled, a percentage of the sampled data points equal to the probability associated with the prediction limit will exceed the minimum required value.

Equations 1 and 2 provide the formulas for calculating the confidence and prediction limits for a sample of data from the population. There is, however, a certain practical difficulty associated with the use of the confidence and prediction limits in the sense that they open up towards the extremes of the sample data range and are therefore not convenient for programming purposes. The percentile lines which are linear functions at constant offsets from the regression model are much more convenient to use.

$$CL_P = [A + Bx] \pm t_{\hat{\alpha}, \hat{\nu}} \times s_{y^*x} \times \sqrt{\frac{1}{n} + \frac{1}{j} \frac{(x - \bar{x})^2}{\sum (x_i - \bar{x})^2}} \quad (1)$$

Where CL_P = Confidence limit at probability P

A and B = regression coefficients for a linear regression model

x = value of independent variable at which the confidence limit is calculated

$t_{\hat{\alpha}, \hat{\nu}}$ = t-value from students t distribution for $\hat{\alpha} = 1-P$ and $\hat{\nu}$ = degrees of freedom (n-2)

$s_{y|x}$ = standard error of estimate calculated from Equation 1(b)

x_i = i-th known value of the independent variable from the observed data points

(x_i, y_i) for $i = 1$ to n

\bar{x} = mean of the observed values of the independent variable

$$s_{y^*x}^2 = \frac{1}{n-2} \sum (y_i - (A + Bx_i))^2 \quad (1b)$$

Where $s_{y|x}^2$ = error variance about the regression

y_i = i-th known value of the dependent variable from the observed data points

(x_i, y_i) for $i = 1$ to n

$$PL_P = [A + Bx] \pm t_{\hat{\alpha}, \hat{\nu}} \times s_{y^*x} \times \sqrt{1 + \frac{1}{n} + \frac{1}{j} \frac{(x - \bar{x})^2}{\sum (x_i - \bar{x})^2}} \quad (2)$$

Where PL_P is the prediction limit at probability P and the other symbols have the same meaning as in Equations 1 and 1(b).

The first two terms of Equation 1 and 2 (in square brackets) represent a straight line and the confidence and prediction limits are calculated by adding or subtracting the quantity calculated in the third term of the equation from the model value at the value "x" of the independent variable.

The incorporation of approximate design reliability in the SAMDM

A decision was taken to use the percentile lines for each of the data sets used for the development of the transfer functions contained in the SAMDM as an indication of approximate design reliability. These percentile lines were determined at the 5th, 10th, 20th and 50th percentile levels for each set of transfer functions implying that 95, 90, 80 and 50 per cent of the data points from the samples used for the development of the transfer functions would lie above these percentile lines. The percentile lines were then used for the design of the pavements contained in the TRH4 pavement design catalogue for the four road categories given in Table 1.

THE CONTENT OF AND PROCEDURE FOLLOWED BY THE SAMDM

Material Characterization for the Current SAMDM

The standard road building materials for South Africa as discussed in TRH14 (1985): Guidelines for Road Construction Materials (5) are listed in Table 2 with their material codes. The suggested stiffness values contained in this section should only serve as a guideline to be used in the absence of laboratory or field measured values or to validate values obtained from laboratory and/or field testing. It is strongly recommended that materials should be tested in the laboratory for individual design cases.

Note: GM = Grading Modulus

$$GM = \frac{P_{2,000mm} \% P_{0,425mm} \% P_{0,075mm}}{100}$$

Where $p_{2,000 \text{ mm}}$ etc. denotes the percentage retained on the indicated sieve size

Hot-mix asphalt material

Freeme (6) suggested the elastic moduli for hot-mix asphalt layers listed in Table 3. Jordaan (7) suggested the values listed in Table 4 based on elastic moduli back-calculated from Multi-depth Deflectometer (MDD) deflection measurements. These values are considerably less than the values listed by Freeme due to the fact that the second set of values was obtained from back-calculation of field deflections. There is still some uncertainty over which approach to use (laboratory versus field values) and the values listed by Freeme are still preferred until the issue is resolved. The value used for the Poisson's Ratio of asphalt material is assumed to be 0.44 in the absence of a measured value.

Granular material

The suggested elastic moduli for granular material are listed in Table 5 (Jordaan (7) and De Beer (8)). The value used for the Poisson's Ratio of granular material is 0.35.

Lightly cemented material

Table 6 contains the suggested elastic moduli values for lightly cemented material in different phases of material behaviour after De Beer (8). The value used for the Poisson's Ratio of cemented material is 0.35. Only the traffic associated deterioration phases of lightly cemented material, phase 1 and phase 2 to the right of the dotted line in Table 6, are included for modelling in the SAMDM. Phase 1 of the traffic associated distress is, however, modelled with the stiffness values at the beginning of this phase which corresponds to the stiffness values given for the post-construction deterioration stage 2. The stiffness input values for a C3 lightly cemented material during phase 1 traffic associated deterioration will therefore be between 1000 and 2000 Mpa although the average stiffness of this material during phase 1 will be between 500 and 800 MPa.

TABLE 2: South African road-building materials with their material codes

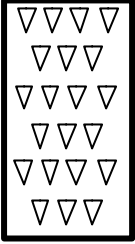
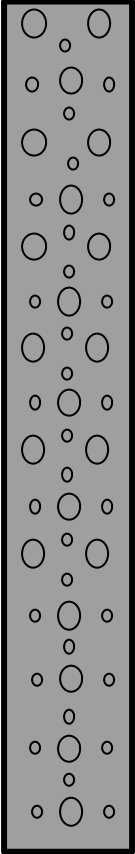
Symbol	Code	Material	Abbreviated specification
	G1	Graded crushed stone	Dense-graded, unweathered crushed stone; Max size 37,5 mm; 88% apparent density; PI < 4,0 (min 6 tests)
	G2	Graded crushed stone	Dense-graded crushed stone; Max size 37,5 mm; 100 - 102 % mod. AASHTO or 85% bulk density; PI < 6,0 (min 6 tests)
	G3	Graded crushed stone	Dense-graded crushed stone and soil binder; max size 37,5 mm; 98 - 100% mod. AASHTO; PI < 6
	G4	Natural Gravel	CBRÛ 80; max size 53 mm; 98 - 100 mod. AASHTO; PI < 6; Swell 0,2 @ 100 % mod. AASHTO
	G5	Natural Gravel	CBRÛ 45; max size 63 mm or b of layer thickness; density as prescribed for layer of usage; PI < 10; Swell 0,5 @ 100 % mod. AASHTO
	G6	Natural Gravel	CBRÛ 25; max size 63 mm or b of layer thickness; density as prescribed for layer of usage; PI < 12 or 2(GM)+10; Swell 1,0 @ 100 % mod. AASHTO
	G7	Gravel-soil	CBRÛ 15; max size b of layer thickness; density as prescribed for layer of usage; PI < 12 or 2(GM)+10; Swell 1,5 @ 100 % mod. AASHTO
	G8	Gravel-soil	CBRÛ 10 at in-situ density; max size b of layer thickness; density as prescribed for layer of usage; PI < 12 or 2(GM)+10; Swell 1,5 @ 100 % mod. AASHTO
	G9	Gravel-soil	CBRÛ 7 at in-situ density; max size b of layer thickness; density as prescribed for layer of usage; PI < 12 or 2(GM)+10; Swell 1,5 @ 100 % mod. AASHTO
	G10	Gravel-soil	CBRÛ 3 at in-situ density; max size b of layer thickness; density as prescribed for layer of usage or 90% mod. AASHTO

TABLE 2: South African road-building materials with their material codes (continued)



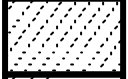

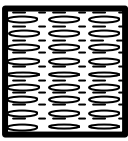
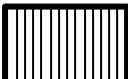

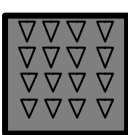

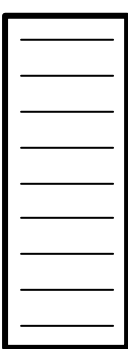
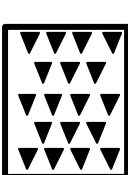
Symbol	Code	Material	Abbreviated specification
	C1	Cemented crushed stone or	UCS 6 - 12 MPa at 100 % mod. AASHTO compaction; at least G2 before treatment
	C2	Cemented crushed stone or	UCS 3 - 6 MPa at 100 % mod. AASHTO compaction; at least G2/G4 before treatment
	C3	Cemented natural gravel	UCS 1,5 - 3,0 MPa and ITS \$ 250 kPa at 100 % mod. AASHTO; max size 63 mm; PI # 6 after treatment
	C4	Cemented natural gravel	UCS 0,75 - 1,5 MPa and ITS \$ 200 kPa at 100 % mod. AASHTO; max size 63 mm; PI # 6 after treatment
	EBM	Bitumen emulsion modified gravel	0,6 - 1,5 % residual bitumen
	EBS	Bitumen emulsion	1,5 - 5,0 % residual bitumen
	BC1	Hot-mix asphalt	Continuously graded; max size 53 mm
	BC2	base course	Continuously graded; max size 37,5 mm
	BC3		Continuously graded; max size 26,5 mm
	BS		Semi-gap graded; max size 37,5 mm
	PPC	Portland concrete cement	Modulus of rupture \geq 4,5 MPa; max particle size \leq 75 mm
	AG	Asphalt surfacing	Gap graded
	AC	layers	Continuously graded
	AS		Semi-gap graded
	AO		Open graded
	AP		Porous (drainage) asphalt
	S1	Surface seals	Single seal
	S2		Multiple seal
	S3		Sand seal
	S4		Cape seal
	S5		Slurry seal; fine grading
	S6		Slurry seal; medium grading
	S7		Slurry seal; course grading
	S8		Rejuvenator
	S9		Diluted emulsion
	WM1	Waterbound and	Max size 75 mm, PI \leq 6, 88 - 90% of apparent density
	WM2	Penetration	Max size 75 mm, PI \leq 6, 86 - 88% of apparent density
	PM	Macadam	Course stone, keystone and bitumen
	DR	Dumprock	Upgraded waste rock, max size \leq of layer thickness

TABLE 3: Elastic Moduli for Asphalt Hot-mix Layers suggested by Freeme (6)

Material grading	Depth from surface (mm)	Stiffness values (MPa) based on temperature and material condition					
		Good condition or new material		Stiff, dry mixture		Very cracked condition	
		20E C	40E C	20E C	40E C	20E C	40E C
Gap-graded	0 - 50	4000	1500	5000	1800	1000	500
	50 - 150	6000	3500	7000	4000	1000	500
	150 - 250	7000	5500	8000	6000	1000	500
Continuously graded	0 - 50	6000	2200	7000	4000	750	500
	50 - 150	8000	5500	9000	6000	1000	750
	150 - 250	9000	7500	10000	8000	1000	750

TABLE 4: Elastic Moduli for Asphalt Layers suggested by Jordaan (7)

Material grading	Depth from surface (mm)	Stiffness values (MPa) based on temperature and material condition					
		Good condition or new material		Stiff, dry mixture		Very cracked condition	
		20E C	40E C	20E C	40E C	20E C	40E C
Gap-graded	0 - 50	1000	200	2000	300	600	200
	50 - 150	2000	300	3000	400	750	300
	150 - 250	3000	400	4000	500	800	400
Continuously graded	0 - 50	2000	300	3000	300	750	300
	50 - 150	4000	400	5000	600	800	400
	150 - 250	6000	1000	7000	1500	1000	750

TABLE 5: Suggested ranges of elastic moduli for granular materials (MPa) with expected values indicated in brackets

Material Code	Material Description	Over cemented layer in slab state	Over granular layer or equivalent	Wet condition (good support)	Wet condition (poor support)
G1	High quality crushed stone	250 - 1000 (450)	150 - 600 (300)	50 - 250 (250)	40 - 200 (200)
G2	Crushed stone	200 - 800 (400)	100 - 400 (250)	50 - 250 (250)	40 - 200 (200)
G3	Crushed stone	200 - 800 (350)	100 - 350 (230)	50 - 200 (200)	40 - 150 (150)
G4	Natural gravel (base quality)	100 - 600 (300)	75 - 350 (225)	50 - 200 (200)	30 - 150 (150)
G5	Natural gravel	50 - 400 (250)	40 - 300 (200)	30 - 150 (150)	20 - 120 (120)
G6	Natural gravel (sub-base quality)	50 - 200 (200)	30 - 200 (150)	20 - 150 (150)	20 - 120 (120)

Selected and in situ subgrade material

The suggested elastic moduli for selected and in situ subgrade material are listed in Table 7 (7). The value used for the Poisson's Ratio of these material is 0.35.

TABLE 7: Suggested elastic moduli for selected and in situ subgrade material (MPa)

Material Code	Soaked CBR	Material Description	Suggested elastic moduli	
			Dry condition	Wet condition
G7	\$ 15	Gravel - Soil	30 - 200	20 - 120
G8	\$ 10	Gravel - Soil	30 - 180	20 - 90
G9	\$ 7	Soil	30 - 140	20 - 70
G10	\$ 3	Soil	20 - 90	10 - 45

Structural Analysis

The structural analysis is normally done with a static, linear elastic multi layer analysis program. A few points related to the structural analysis that will influence the design procedure should be noted.

The maximum horizontal tensile strain at the bottom of asphalt layers and the maximum tensile strain at the bottom of cemented layers are used as the critical parameters determining the fatigue life of these two material types. The position of the maximum tensile strain in a particular layer will not necessarily occur at the bottom of the layer (9,10). The position of the maximum horizontal strain will rather be determined by the modular ratios of the layers in the pavement structure. The transfer functions for these materials were however, developed as a function of tensile strain at the bottom of the layer and are used as such.

Very often, the structural analysis of a pavement with a granular base and subbase will result in the mechanistic design method predicting almost no resistance against shear failure in the subbase layer. This is caused by the linear elastic material models used in the static, linear elastic multi-layer solution procedure which allows tensile stresses to develop in unbound material. The occurrence of tensile stress in a granular layer is again determined by the modular ratio of the stiffness of the granular layer in relation to stiffness of the immediate support layer (11,12). The linear elastic model and the resulting Möhr stress circle for such a case is illustrated in Figure 5.

An interim solution is not to allow any tensile stress to develop in granular materials. If a tensile minor principle stress is calculated in a granular material, the value is set equal to zero. What this implies in practice is that the granular layer will only carry loading in compression. If the minor principle stress is set equal to zero, a re-arrangement of stresses will take place to transfer the loads by compression. The major principle stress is therefore adjusted under the condition that the deviator stress remain constant. The Möhr circle is in effect shifted by this procedure as indicated in Figure 6. Although this tentative adjustment of stresses has not been proven theoretically, it does provide more meaningful pavement designs compared to proven practice. The ultimate solution would, however, be to use a material model as illustrated in Figure 6 rather than the model in Figure 5. However, current linear elastic analysis packages do not allow for such material models and research is being conducted on the finite element analysis of pavement structures with no tension allowed in granular materials.

TABLE 6: Suggested elastic moduli values for cemented material

Original Code	UCS (MPa) for pre-cracked condition	Parent Material Code	Post-construction deterioration		Traffic associated deterioration			
			Stage 1: Intact (GPa)	Stage 2: Shrinkage cracking (MPa)	Phase 1	Phase 2		
					Stage 3: Traffic associated cracking, transitional phase with micro cracking (MPa)	Stage 4: Broken up in equivalent granular state (MPa)		
						Dry condition	Wet condition	Equivalent code
C1	6 - 12	Crushed stone G1	6 - 30	2500 - 3000	800 - 1000	400 - 600	50 - 400	EG1
		Crushed stone G3						EG2
C2	3 - 6	Crushed stone G2	3 - 14	2000 - 2500	500 - 800	300 - 500	50 - 300	EG2
		Crushed stone G3						EG3
		Gravel G4						EG4
C3	1,5 - 3	Gravel G4	2 - 10	1000 - 2000	500 - 800	200 - 400	20 - 200	EG4
		Gravel G5						EG5
		Gravel G6						EG6
		Gravel G7						EG7
		Gravel G8						EG8
C4	0.75 - 1.5	Gravel G4	0.5 - 7	500 - 2000	400 - 600	100 - 300	20 - 200	EG4
		Gravel G5						EG5
		Gravel G6						EG6
		Gravel G7						EG7
		Gravel G8						EG8
		Gravel G7						EG9
Gravel G8	EG10							

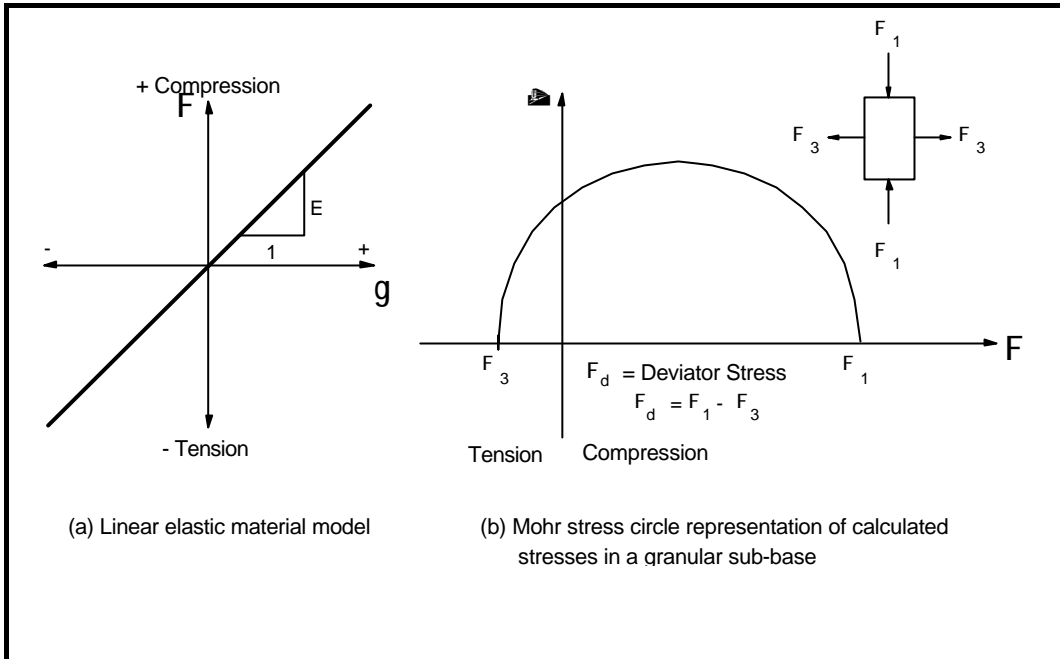


Figure 5: Conventional linear elastic material model with the resulting stress state in granular subbases

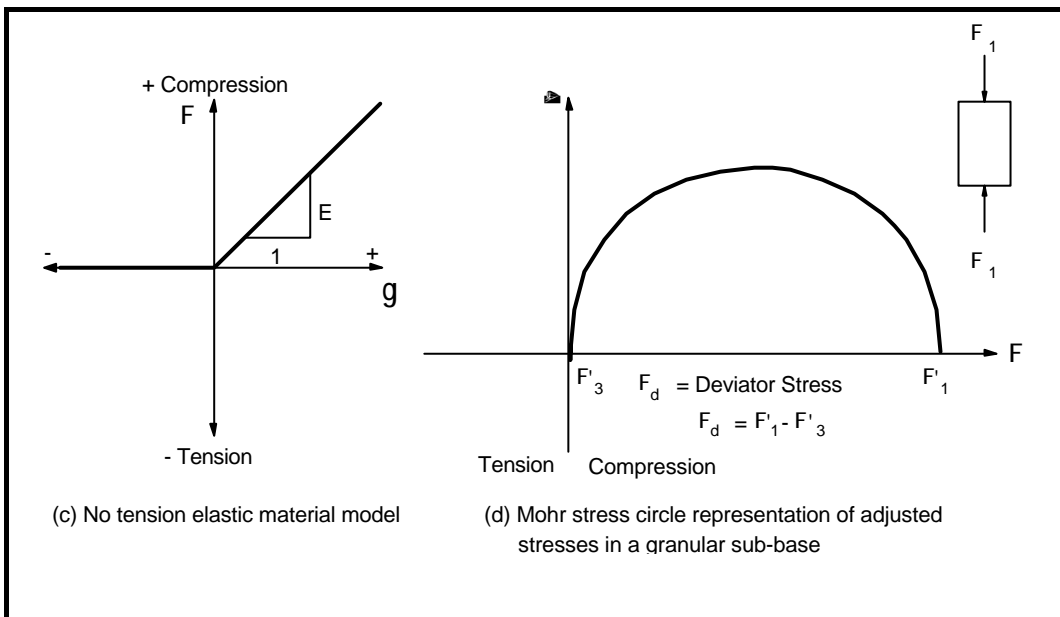


Figure 6: Suggested bi-linear elastic material model with the resulting stress state in granular subbases

Pavement Bearing Capacity Estimation

The SAMDM is in essence a critical layer approach whereby the most critical layer will determine the bearing capacity of the pavement structure. There are three concepts involved in the process of estimating pavement bearing capacity. The first is to estimate the bearing capacity of the individual layers in the pavement structure. Secondly, the occurrence of crushing in cemented layers should be investigated and thirdly the estimated bearing capacity of the pavement should be calculated from the values for the individual layers.

Reference is often made to the “life” of a layer when referring to the number of load repetitions that the layer can sustain before reaching a terminal condition. This is not strictly correct as the mechanistic method does not predict layer and pavement life. The term layer life will, however, be used in this document as a convenient way of referring to the bearing capacity of a layer.

Failure modes, critical parameters and transfer functions for pavement materials

The basic material types used in South Africa are asphalt, granular, cemented and subgrade materials. Each material type exhibits a unique mode of failure. The failure mode for each material type is linked to a critical parameter calculated at a specific position in the pavement structure under loading. Transfer functions provide the relationship between the value of the critical parameter and the number of load applications that can be sustained at that value of the critical parameter, before the particular material type will fail in a specific mode of failure. The following sections will describe each basic material type with its accompanying critical parameter(s), mode(s) of failure and applicable transfer function(s).

Hot-mix asphalt material

The classical model of fatigue failure is used for hot-mix asphalt where this material fails due to fatigue cracking under repeated loading as a result of tensile strain \hat{a}_t ($\mu\hat{a}$) at the bottom or in the layer. A distinction is made between thin asphalt surfacing layers (<50 mm) and thick asphalt bases (>75 mm). Transfer functions are provided for a continuously graded or gap-graded surfacing layer and asphalt base layers with stiffness values varying from 1000 MPa to 8000 MPa.

Continuously graded asphalt surfacing layers

The fatigue crack initiation transfer functions for continuously graded material at different service levels are listed in Equations 3 to 6 (13) and illustrated in Figure 7.

$$N_f = 10^{17.40 \left(1 + \frac{\text{Log } \hat{a}_t}{3.40}\right)} \quad \text{for category A roads} \quad (3)$$

$$N_f = 10^{17.46 \left(1 + \frac{\text{Log } \hat{a}_t}{3.41}\right)} \quad \text{for category B roads} \quad (4)$$

$$N_f = 10^{17.54 \left(1 + \frac{\text{Log } \hat{a}_t}{3.42}\right)} \quad \text{for category C roads} \quad (5)$$

$$N_f = 10^{17.71 \left(1 + \frac{\text{Log } \hat{a}_t}{3.46}\right)} \quad \text{for category D roads} \quad (6)$$

Gap-graded asphalt surfacing layers

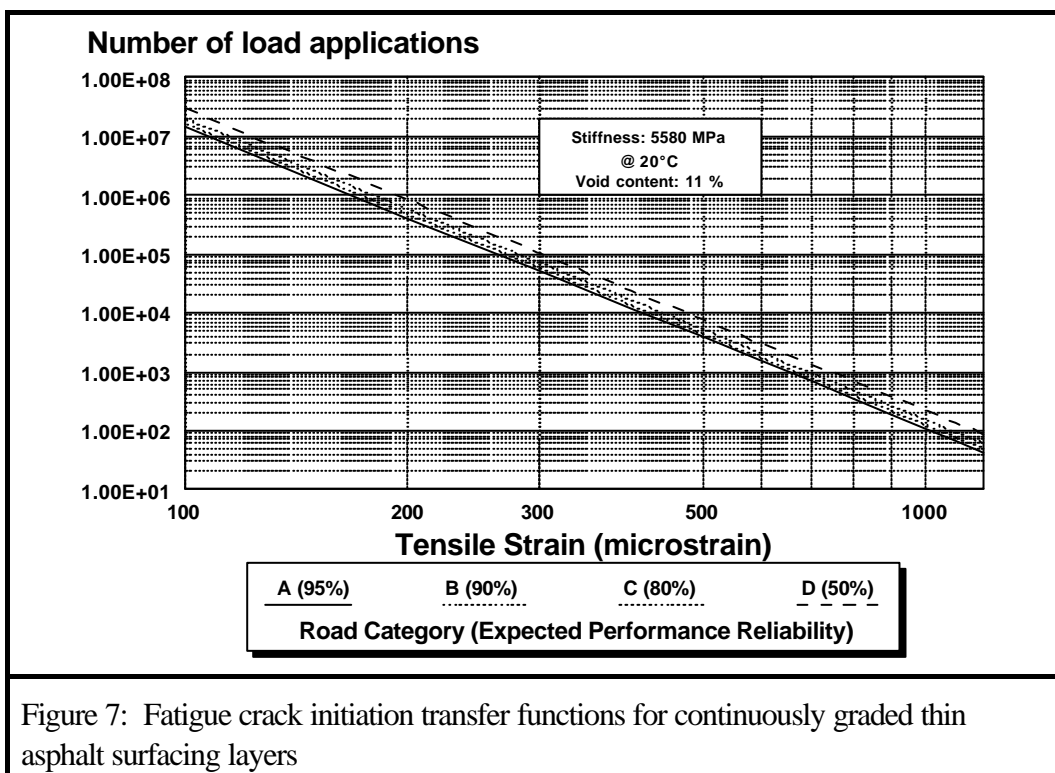
The fatigue crack initiation transfer functions for gap graded material at different service levels are listed in Equations 7 to 10 (13) and illustrated in Figure 8.

$$N_f = 10^{15.79 \left(1 + \frac{\log \dot{a}_t}{3.71}\right)} \quad \text{for category A roads} \quad (7)$$

$$N_f = 10^{15.85 \left(1 + \frac{\log \dot{a}_t}{3.72}\right)} \quad \text{for category B roads} \quad (8)$$

$$N_f = 10^{15.93 \left(1 + \frac{\log \dot{a}_t}{3.74}\right)} \quad \text{for category C roads} \quad (9)$$

$$N_f = 10^{16.09 \left(1 + \frac{\log \dot{a}_t}{3.77}\right)} \quad \text{for category D roads} \quad (10)$$



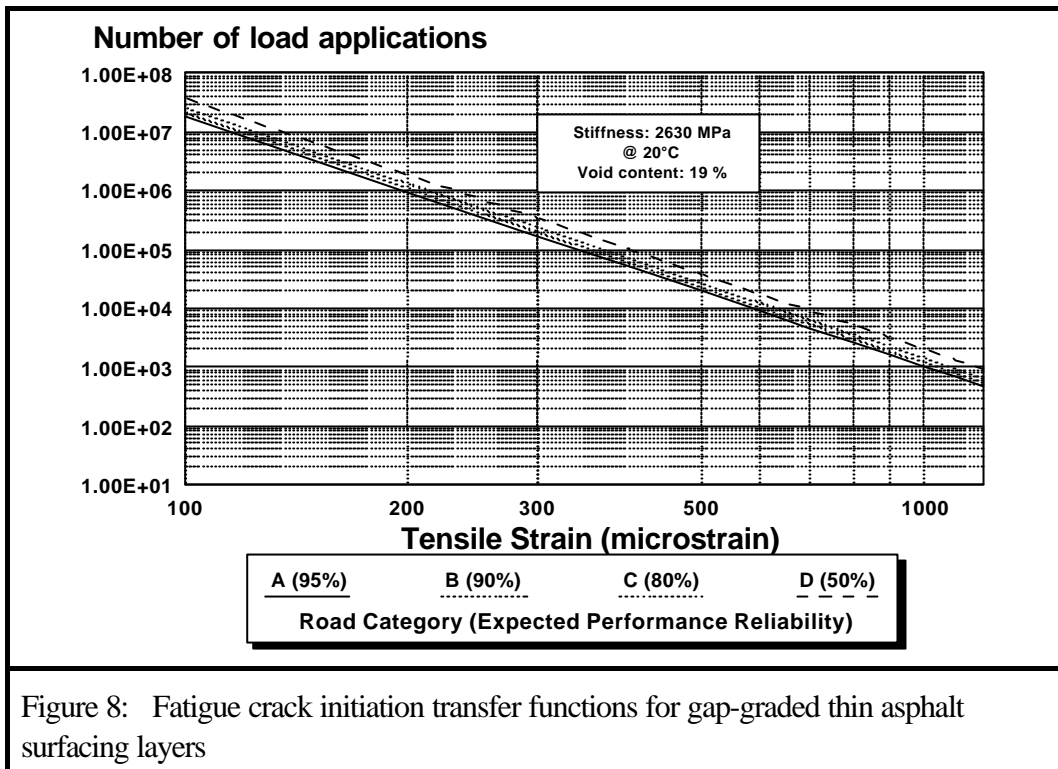


Figure 8: Fatigue crack initiation transfer functions for gap-graded thin asphalt surfacing layers

Thick Asphalt Bases

The general form of the fatigue crack initiation transfer functions for thick asphalt bases, is given in Equation 11 (13). Table 8 (13) contains the regression coefficients for Equation 11, for combinations of road category and approximate asphalt hot-mix stiffness. Figure 9 to 13 illustrates the fatigue crack initiation transfer functions for different approximate asphalt hot-mix stiffness values.

$$N_f = 10^{A \left(1 + \frac{\text{Log } \dot{\epsilon}_t}{B}\right)} \quad \text{for all road categories} \quad (11)$$

TABLE 8: Regression coefficients for the general fatigue crack initiation transfer function for thick asphalt bases

Hot-mix asphalt stiffness (MPa)	Road Category/ Service level	A	B
1000	A	16.44	3.378
	B	16.81	3.453
	C	17.25	3.543
	D	17.87	3.671
2000	A	16.09	3.357
	B	16.43	3.428
	C	16.71	3.487
	D	17.17	3.583

TABLE 8: Regression coefficients for the general fatigue crack initiation transfer function for thick asphalt bases (continued)

Hot-mix asphalt stiffness (MPa)	Road Category/ Service level	A	B
3000	A	15.78	3.334
	B	16.11	3.403
	C	16.26	3.435
	D	16.68	3.524
5000	A	15.52	3.317
	B	15.73	3.362
	C	15.83	3.383
	D	16.10	3.441
8000	A	15.09	3.227
	B	15.30	3.272
	C	15.39	3.291
	D	15.65	3.346

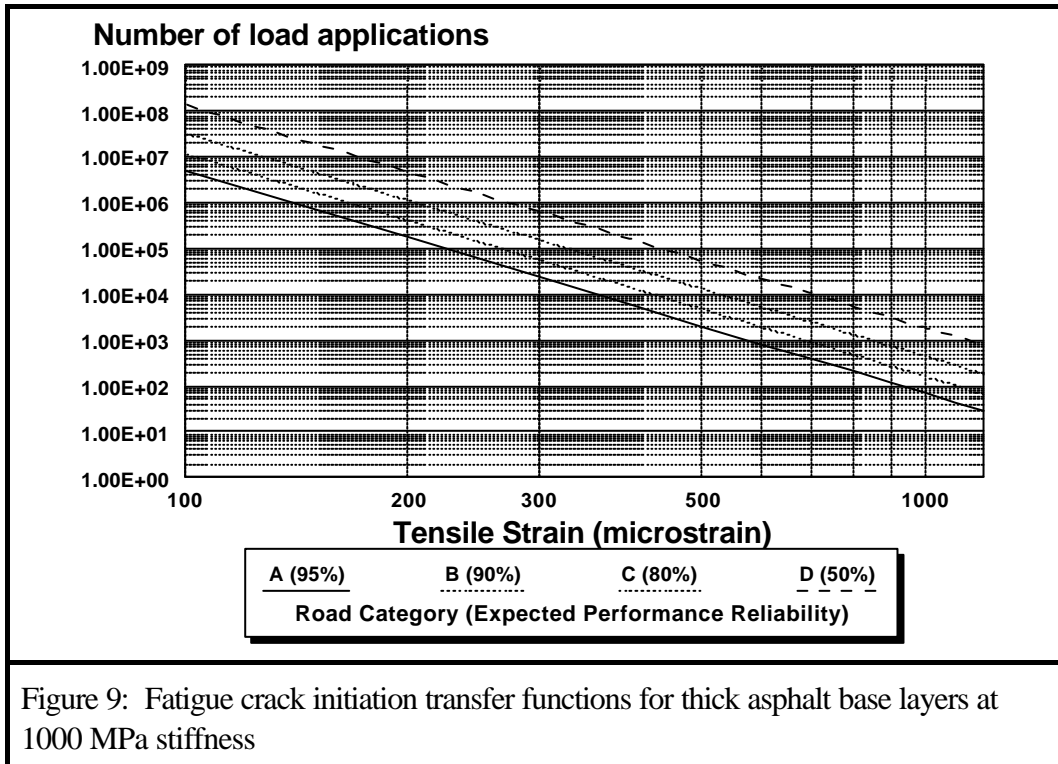


Figure 9: Fatigue crack initiation transfer functions for thick asphalt base layers at 1000 MPa stiffness

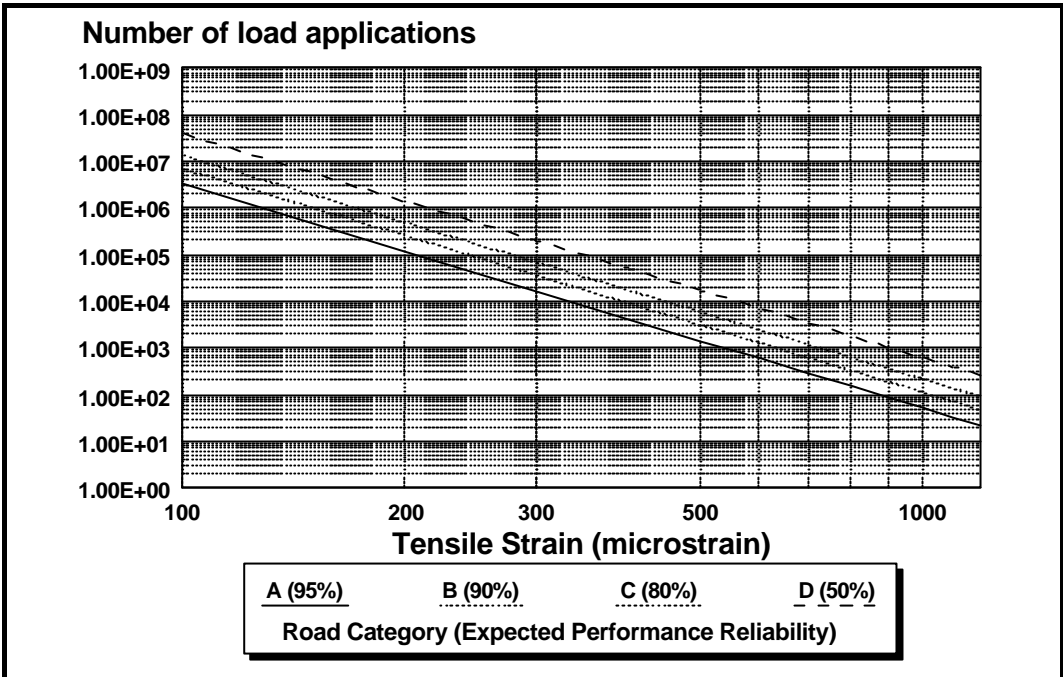


Figure 10: Fatigue crack initiation transfer functions for thick asphalt base layers at 2000 MPa stiffness

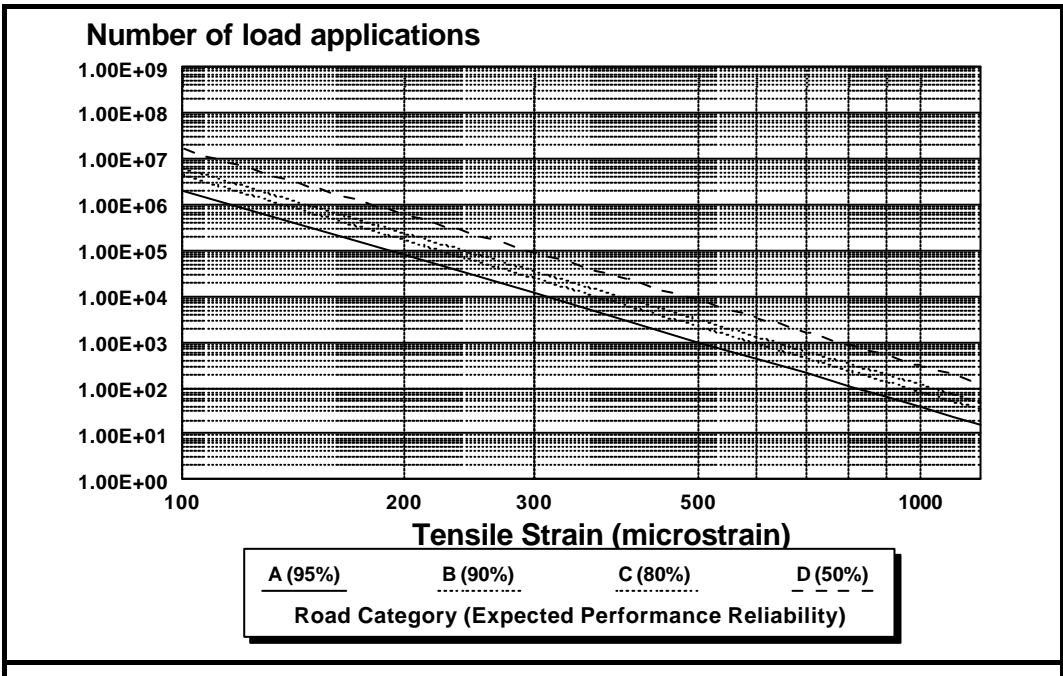


Figure 11: Fatigue crack initiation transfer functions for thick asphalt base layers at 3000 MPa stiffness

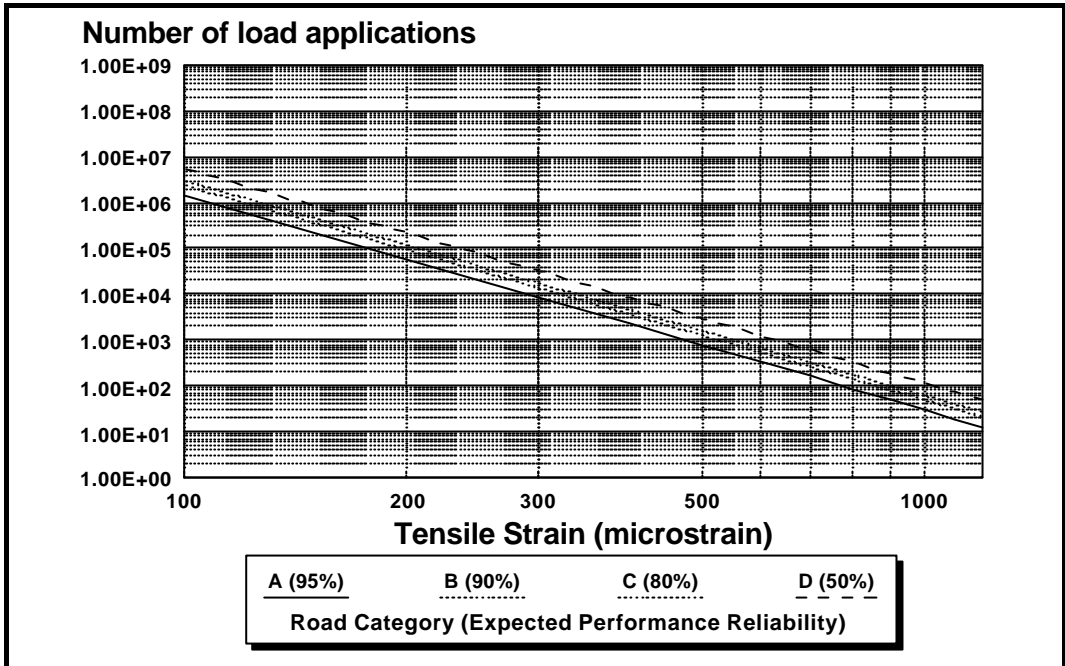


Figure 12: Fatigue crack initiation transfer functions for thick asphalt base layers at 5000 MPa stiffness

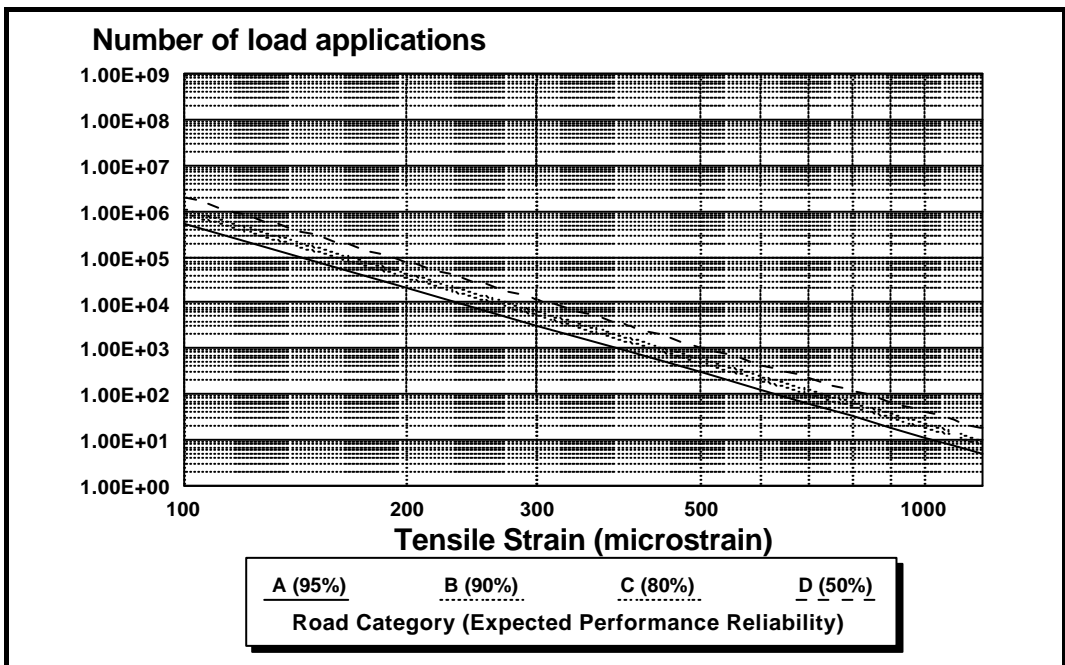


Figure 13: Fatigue crack initiation transfer functions for thick asphalt base layers at 8000 MPa stiffness

Figure 16 illustrates the shift factor to convert the crack initiation life to the total fatigue life after surface cracks appear on the road surface. The total asphalt depth should be considered to determine the shift factor.

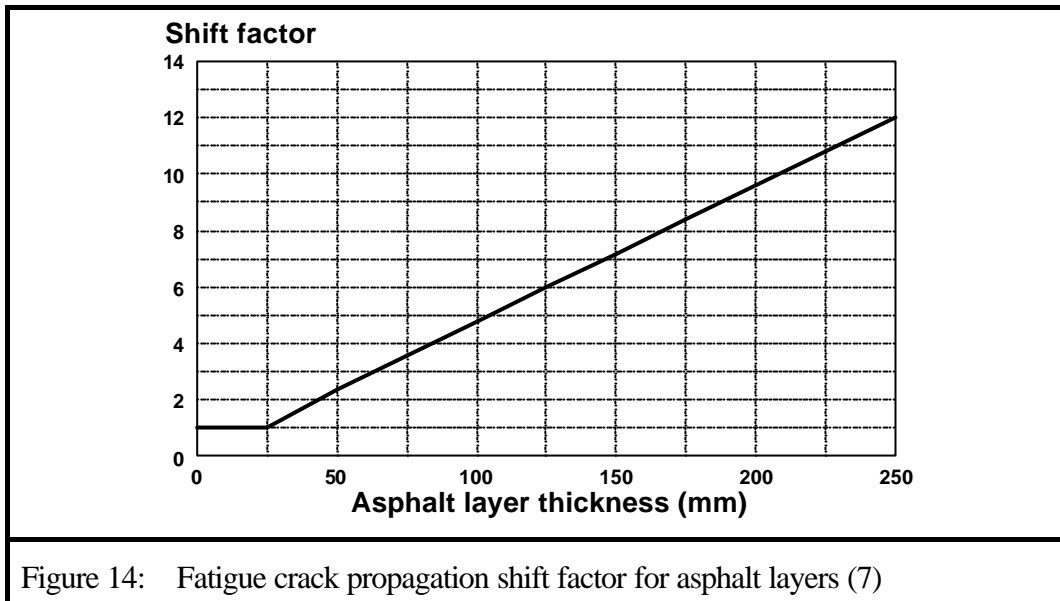


Figure 14: Fatigue crack propagation shift factor for asphalt layers (7)

Granular Material

Granular material exhibits deformation due to densification and gradual shear under repeated loading. Maree (14) developed the concept of the "safety factor" against shear failure for granular materials. The safety factor concept was developed from Mohr-Coulomb theory and represents the ratio of the material shear strength divided by the applied stress causing shear. The safety factor was then correlated with the gradual permanent deformation of granular material under dynamic triaxial loading at specific levels of the safety factor.

The safety factor against shear failure for granular materials is defined by

$$F = \frac{\sigma_3 [K (\tan^2(45^\circ + \frac{\phi}{2})) + 1] + 2KC \tan(45^\circ + \frac{\phi}{2})}{(\sigma_1 \& \sigma_3)} \tag{12}$$

or

$$F = \frac{\sigma_3 \phi_{term} + c_{term}}{(\sigma_1 \& \sigma_3)} \tag{13}$$

where σ_1 and σ_3 = major and minor principle stresses acting at a point in the granular layer (compressive stress positive and tensile stress negative)

C = cohesion

ϕ = angle of internal friction

K = constant = 0.65 for saturated conditions

0.8 for moderate moisture conditions and

0.95 for normal moisture conditions

Safety factors smaller than 1 imply that the shear stress exceeds the shear strength and that rapid shear failure will occur for the static load case. Under real life dynamic loading the shear stress will only exceed the shear strength for a very short time and shear failure will not occur under one load application, but shear deformation will rapidly accumulate under a number of load repetitions. If the safety factor is larger than 1, deformation will accumulate gradually with increasing load applications. In both instances the mode of failure will however, be the deformation of the granular layer and the rate of deformation is controlled by the magnitude of the safety factor against shear failure.

The safety factor or the major and minor principle stresses are referred to as the critical parameters for granular layers for the purpose of this paper. The major and minor principle stresses and hence the safety factor are usually calculated at the mid-depth of granular layers. Suggested values of the C and ö-terms for granular materials are given in Table 9. The transfer functions, relating the safety factor to the number of load applications that can be sustained at that safety factor level, are given by Equations 14 to 17 (13) for different service level requirements and are illustrated in Figure 15.

TABLE 9: Suggested C_{term} and \ddot{o}_{term} values for granular material (modified from ref 6)

Material Code	Moisture Condition					
	Dry		Moderate		Wet	
	ö-term	C-term	ö-term	C-term	ö-term	C-term
G1	8.61	392	7.03	282	5.44	171
G2	7.06	303	5.76	221	4.46	139
G3	6.22	261	5.08	188	3.93	115
G4	5.50	223	4.40	160	3.47	109
G5	3.60	143	3.30	115	3.17	83
G6	2.88	103	2.32	84	1.76	64
EG4	4.02	140	3.50	120	3.12	100
EG5	3.37	120	2.80	100	2.06	80
EG6	1.63	100	1.50	80	1.40	60

$$N_A = 10^{(2.605122F - 3.480098)} \quad \text{for category A roads} \quad (14)$$

$$N_B = 10^{(2.605122F - 3.707667)} \quad \text{for category B roads} \quad (15)$$

$$N_C = 10^{(2.605122F - 3.983324)} \quad \text{for category C roads} \quad (16)$$

$$N_D = 10^{(2.605122F - 4.510819)} \quad \text{for category D roads} \quad (17)$$

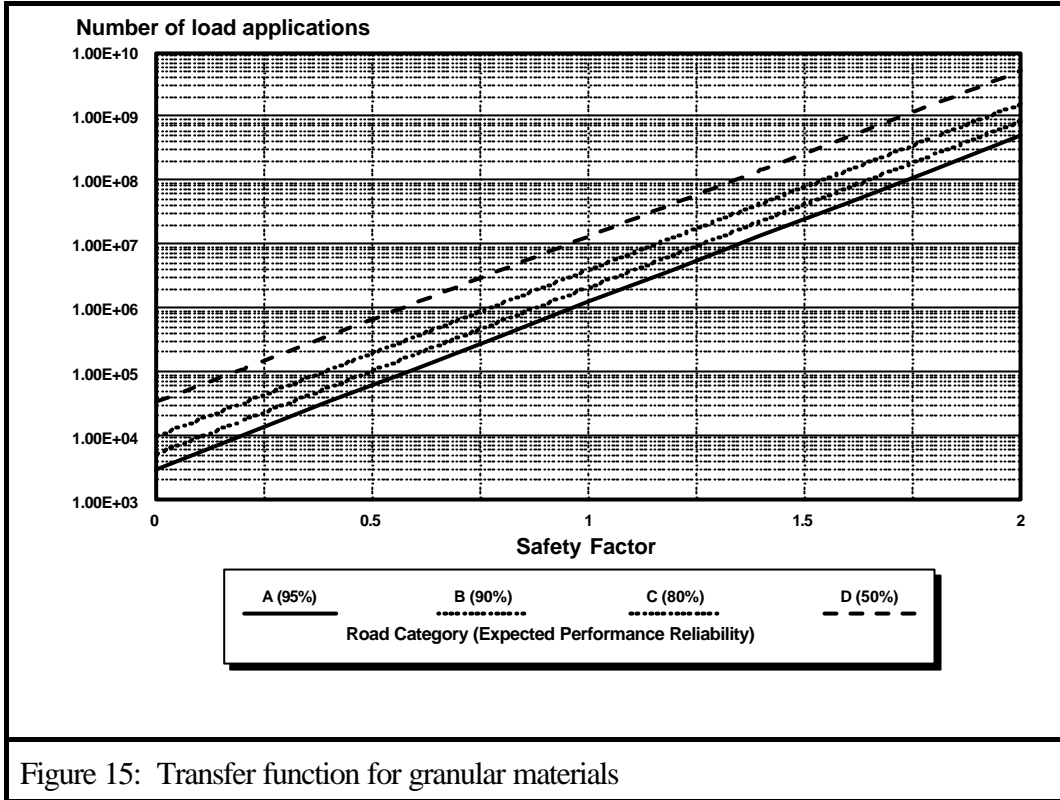


Figure 15: Transfer function for granular materials

Cemented Material

Cemented material exhibits two failure modes, namely effective fatigue and crushing (15). The critical parameters for cemented material are the maximum tensile strain \hat{a} ($\mu\hat{a}$), at the bottom or in the layer for controlling the effective fatigue life and the vertical compressive stress $\hat{\sigma}_v$ (kPa), on top of the cemented layer controlling the crushing life. Transfer functions are provided for two crushing conditions, namely crush initiation with roughly 2 mm deformation on top of the layer and advanced crushing with 10 mm deformation and extensive breakdown of the cemented material.

Equations 18 to 21 (13) contain equations for the effective fatigue transfer functions at different service levels of cemented materials as a function of the tensile strain \hat{a} ($\mu\hat{a}$), illustrated in Figure 16. The default input values suggested for the strain at break \hat{a}_b ($\mu\hat{a}$) and the Unconfined Compressive Strength UCS (kPa) of cemented materials are given in Table 10.

$$N_{eff} = 10^{6.72(1 + \frac{\hat{a}}{7.49\hat{a}_b})} \quad \text{for category A roads} \quad (18)$$

$$N_{eff} = 10^{6.84(1 + \frac{\hat{a}}{7.63\hat{a}_b})} \quad \text{for category B roads} \quad (19)$$

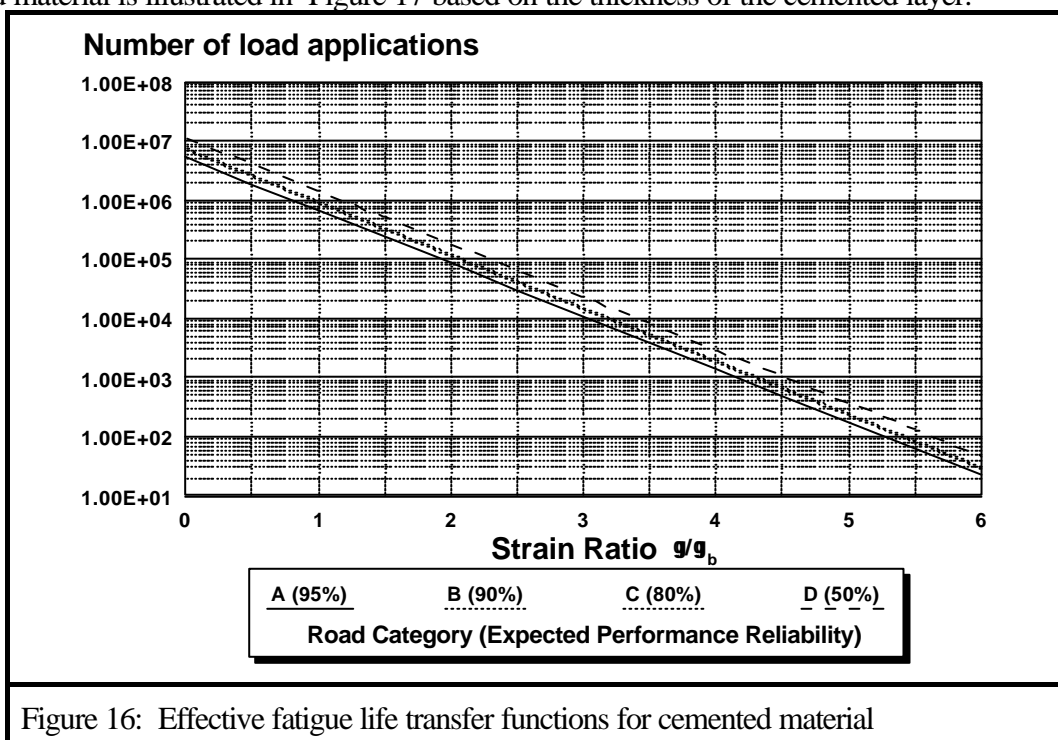
$$N_{eff} = 10^{6.87(1 + \frac{\hat{a}}{7.66\hat{a}_b})} \quad \text{for category C roads} \quad (20)$$

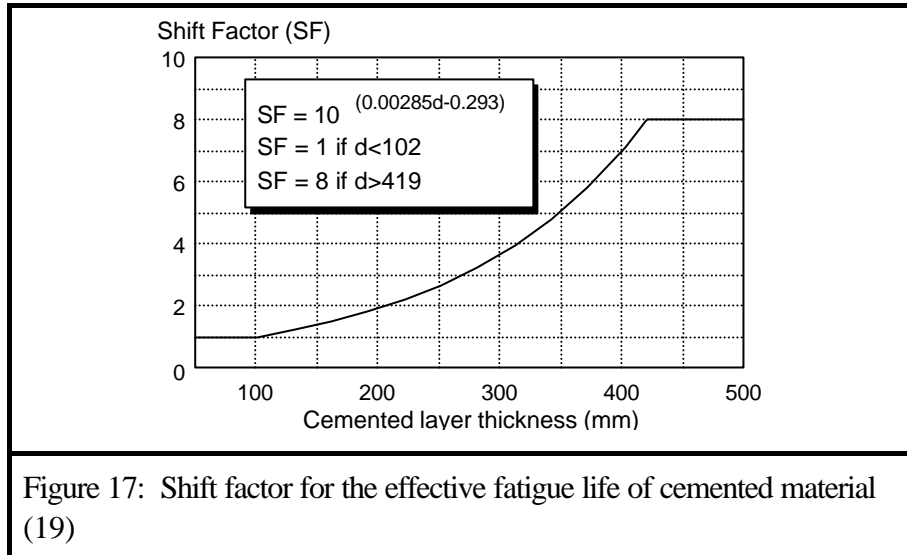
$$N_{eff} = 10^{7.06(1 - \frac{\dot{a}}{7.86\dot{a}_b})} \quad \text{for category D roads} \quad (21)$$

TABLE 10: Suggested values of \dot{a}_b and UCS for Cemented Material

Material code	\dot{a}_b ($\mu\dot{a}$)	UCS (kPa)
C1	145	7500
C2	120	7500
C3	125	2250
C4	145	1125

The transfer functions in Equations 18 to 21 represent the effective fatigue life of the cemented material. At the end of the effective fatigue life of a cemented material, the material is assumed to behave similarly to granular material. These transfer functions do not allow for different layer thicknesses. A shift factor for cemented material was therefore introduced to allow thicker layers to have an extended effective fatigue life compared to thinner layers subjected to the same strain. The shift factor for the effective fatigue life of cemented material is illustrated in Figure 17 based on the thickness of the cemented layer.





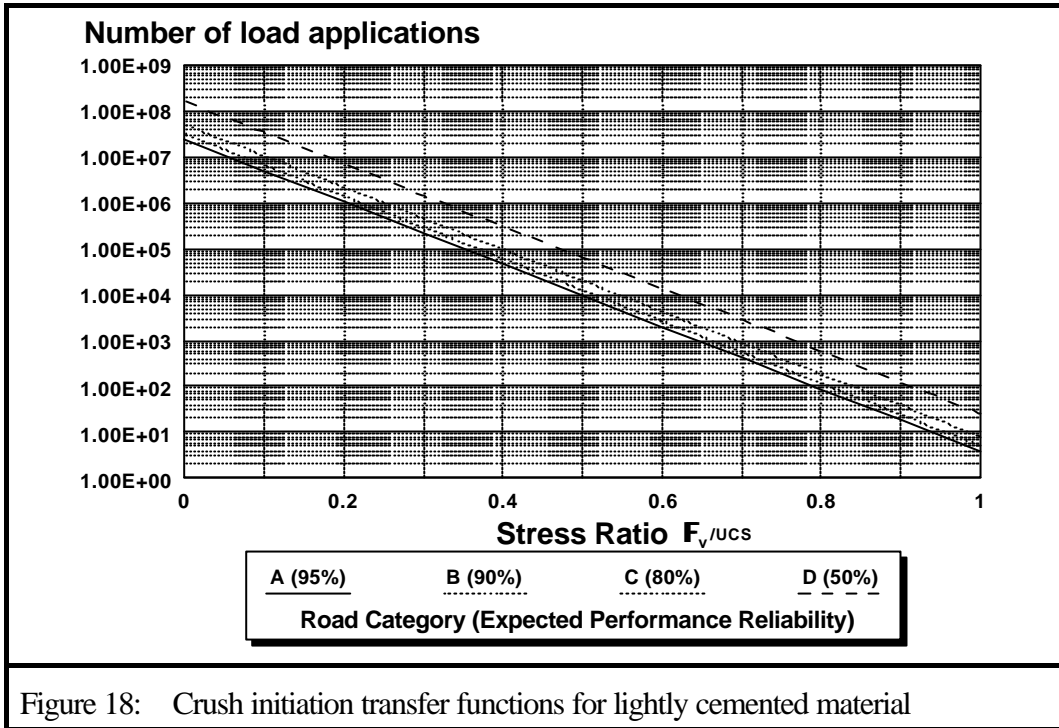
Equations 22 to 25 (13) contain the transfer functions for crush initiation (N_{Ci}) and Equations 26 to 29 (13) the transfer functions for advanced crushing (N_{Ca}) of cemented material, illustrated in Figures 18 and 19 respectively.

$$N_{C_i} = 10^{7.386(1 + \frac{\sigma_v}{1.09 UCS})} \quad \text{for category A roads} \quad (22)$$

$$N_{C_i} = 10^{7.506(1 + \frac{\sigma_v}{1.10 UCS})} \quad \text{for category B roads} \quad (23)$$

$$N_{C_i} = 10^{7.706(1 + \frac{\sigma_v}{1.13 UCS})} \quad \text{for category C roads} \quad (24)$$

$$N_{C_i} = 10^{8.516(1 + \frac{\sigma_v}{1.21 UCS})} \quad \text{for category D roads} \quad (25)$$

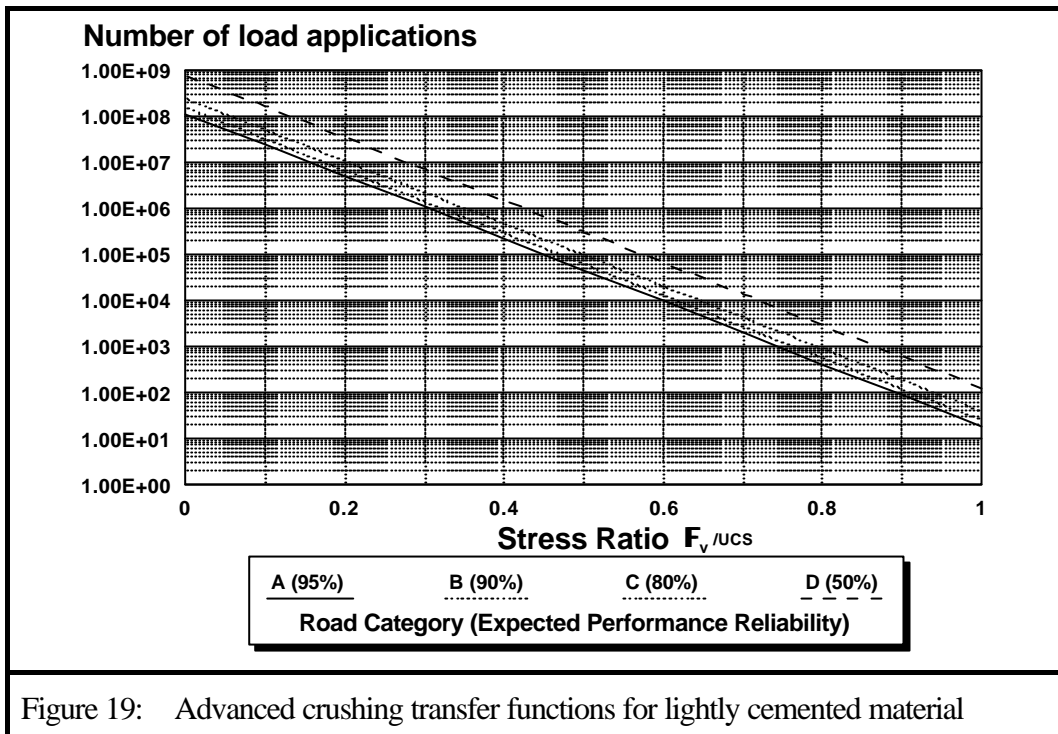


$$N_{C_a} = 10^{8.064(1 + \frac{\sigma_v}{1.19 UCS})} \quad \text{for category A roads} \quad (26)$$

$$N_{C_a} = 10^{8.184(1 + \frac{\sigma_v}{1.2 UCS})} \quad \text{for category B roads} \quad (27)$$

$$N_{C_a} = 10^{8.384(1 + \frac{\sigma_v}{1.23 UCS})} \quad \text{for category C roads} \quad (28)$$

$$N_{C_a} = 10^{8.894(1 + \frac{\sigma_v}{1.31 UCS})} \quad \text{for category D roads} \quad (29)$$



Subgrade material

The mode of failure for the selected and in situ subgrade material is the permanent deformation of these layers, resulting in the deformation of the road surface. The critical parameter for these materials is the vertical strain ($\hat{\epsilon}_v$) at the top of the layer. Transfer functions are provided for two terminal conditions, a 10 mm or a 20 mm surface rut due to the deformation of the subgrade material.

Equation 30 (13) gives the general form of the transfer function for the selected and subgrade material with the regression coefficients for the 10 and 20 mm terminal rut condition listed in Table 11 (13) for different service levels / road categories. The transfer functions for the 10 mm terminal rut condition are illustrated in Figure 20 and those for the 20 mm terminal rut condition in Figure 21.

TABLE 11: Regression coefficients for the subgrade deformation transfer function

Terminal rut condition (mm)	Road Category / Service Level	A
10	A	33.30
	B	33.38
	C	33.47
	D	33.70
20	A	36.30
	B	36.38
	C	36.47
	D	36.70

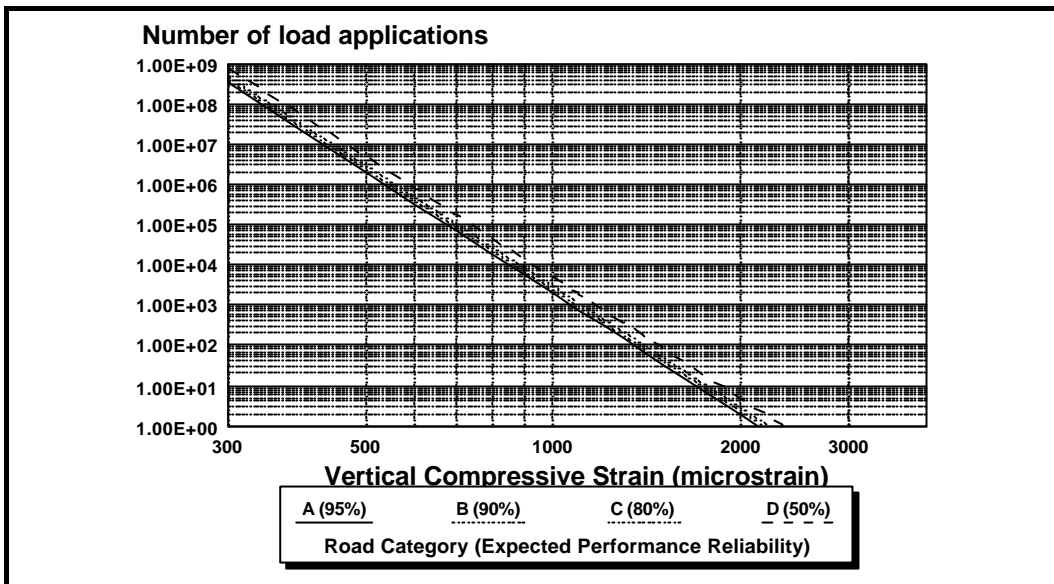


Figure 20: 10 mm Subgrade deformation transfer functions

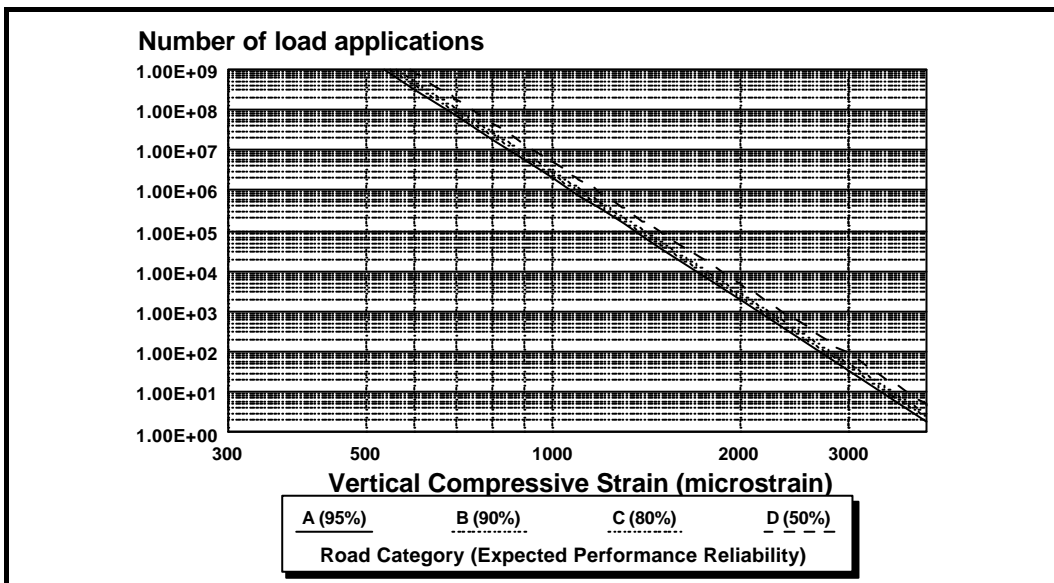


Figure 21: 20 mm Subgrade deformation transfer functions

Incorporation of the crushing failure of cemented material

The crushing failure of cemented material was described by De Beer (15) but has not been included in the South African Mechanistic Design Method to date. The transfer functions for crush initiation and advanced crushing were listed in a previous section.

Figure 22 illustrates the long-term behaviour of a lightly cemented layer in a pavement structure. During the pre-cracked phase, the elastic modulus of the layer will be in the order of 3000 to 4000 MPa and the layer will act as a slab with the slab dimensions a few times larger than the layer thickness. This E-value reduces rapidly to values in the order of 1500 to 2000 MPa (stage 2, Table 6) at the onset of the effective fatigue life

phase. The layer is further broken down from large blocks with dimensions of approximately 1 to 5 times the layer thickness, to particles smaller than the thickness of the layer during the effective fatigue life phase. During the equivalent granular phase, the elastic modulus is in the order of 200 to 300 MPa (stage 4, Table 6) and the cemented material acts typically like a granular layer.

Although these changes in the behaviour of the cemented material will gradually occur with time, they are modelled as stepwise phases in the life of the cemented material. The effective fatigue life phase and the equivalent granular phase of cemented material behaviour is used to calculate the layer life of the cemented layer. The pre-cracked phase is considered to be very short (15) in relation to the other phases and is therefore not included in predicting the layer life for the cemented material.

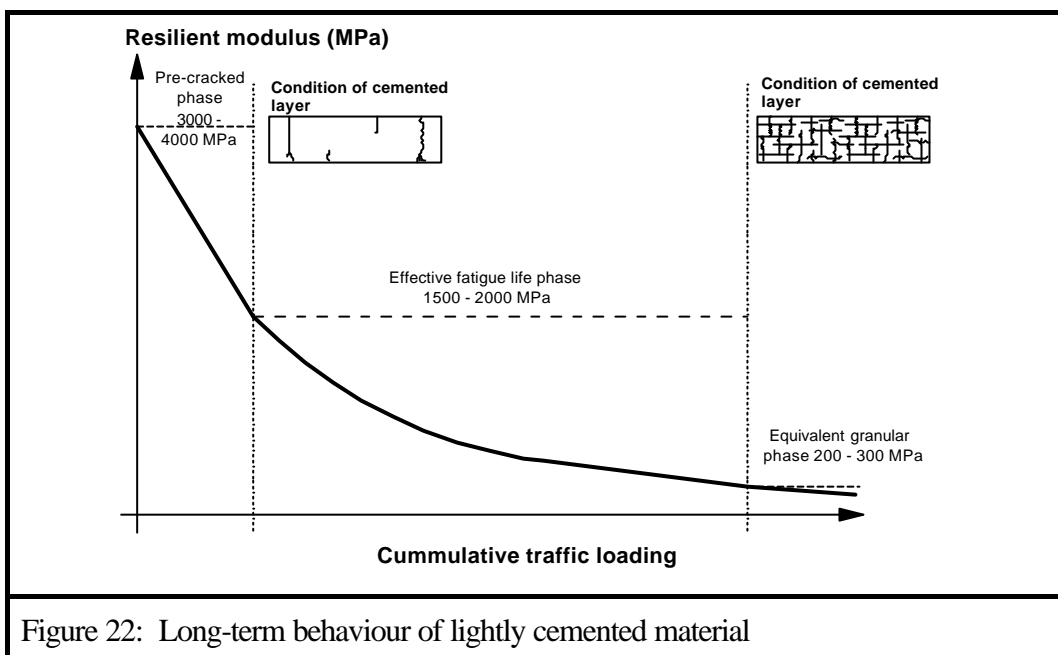


Figure 22: Long-term behaviour of lightly cemented material

Consider a pavement structure with a cemented base and subbase with a stepwise model for the cemented material behaviour. It is clear that at the end of the effective fatigue life phase for the subbase, there will be a sudden change in the elastic modulus of the sub-base, resulting in a re-arrangement of stresses and strains in the pavement structure. The stresses and strains calculated during the effective fatigue life phase will therefore not be valid any more, except for the vertical stress on top of the cemented base which will remain almost the same as this parameter is influenced more by the applied contact stress than the structural conditions below it. This argument allows the concept of crushing failure to be introduced in the South African Mechanistic Design Method. The procedure for determining whether crushing failure will occur is best illustrated by Figure 23.

In Figure 23(b) the granular state is reached in the base before crush initiation or advanced crushing take place. During the equivalent granular stage the modulus of the base is too low to allow crushing to continue to the same extent as for a cemented base. In Figure 23(c) the predicted crush initiation life is shorter than the predicted effective fatigue life and crush initiation will occur with approximately 2 mm deformation on top of the cemented material. In Figure 23(d) the predicted effective fatigue life exceeds both the crush initiation and advanced crushing life and advanced crushing will occur with approximately 10 mm deformation on top of the cemented material as a result.

Crushing is not considered as a critical mode of distress which will limit pavement bearing capacity in the SAMDM. If crushing is flagged as a potential problem, the base layer material quality is increased or more protection is provided against high contact stresses by using a thicker asphalt surfacing layer.

Pavement behaviour phases and the residual life concept

The concept of pavement behaviour phases has already been introduced in the previous section. These phases are caused by changes mostly taking place in the cemented layers of a pavement structure. The modulus of a cemented layer is modelled as a constant value for the duration of a particular phase with a sudden change at the end of each phase.

A single cemented layer therefore introduces two phases to the pavement design model and the rest of the cemented layers one each. For example, a pavement structure with a cemented base and subbase will have a first phase up to the point where the subbase reaches the end of its estimated effective fatigue life. The modulus of the subbase will then suddenly reduce and the cemented base will still be in its effective fatigue life phase for the second phase of pavement behaviour. At the end of the estimated effective fatigue life of the cemented base, the modulus of the base reduces and both the base and the subbase are in an equivalent granular condition for the third and last phase of pavement behaviour. This process is illustrated in Figure 24.

The stresses and strains calculated during one phase, are not valid during the following phase. A structural analysis is therefore done for each phase with the applicable reduced moduli for the cemented layers during the second and subsequent phases of pavement behaviour. The stresses and strains calculated for each phase will yield an estimate of the layer life for each layer during each phase. The transfer functions used for pavement design were however, developed from initial conditions of no distress. After Phase 1, the predicted layer life for both Phase 1 and 2 therefore becomes invalid but by combining the two values, an ultimate layer life may be calculated.

Consider the situation in Figure 25 where the layer life for each layer has been calculated for Phase 1. At the end of Phase 1, the modulus of the cemented layer is suddenly reduced, resulting in higher stress/strain conditions in the other layers similar to the effect of an increase in loading on the pavement. The remaining part of the layer life calculated for the other layers for Phase 1, or the residual life of the other layers, is then reduced because of the increased stress conditions during subsequent phases. The method assumes that the rate of decrease in the residual life of the other layers during the second phase, is equal to the ratio of the Phase 1 layer life divided by the Phase 2 layer life for a particular layer, similar to a load equivalency factor. The only exception is the cemented layer which will start with a clean sheet for the second phase because there is a change in material state and therefore terminal condition for this layer. The calculated equivalent granular layer life for the original cemented layer will therefore be allocated to the life of the cemented layer in total for the second phase. Also note that if the top layer is a surfacing layer such as a surface seal or thin asphalt layer, the calculated layer life for the top layer will not affect the ultimate pavement bearing capacity. The reason for this is that it is not possible to design the thin asphalt surfacing layers for the total structural design life of pavement structures, especially for high design traffic classes and surface maintenance should be done at regular intervals as recommended by the TRH4 document. The ultimate pavement bearing capacity is calculated as the sum of the duration of Phase 1 and the minimum adjusted residual life for Phase 2 or the equivalent granular layer life of the original cemented layer during Phase 2, whichever is the smallest.

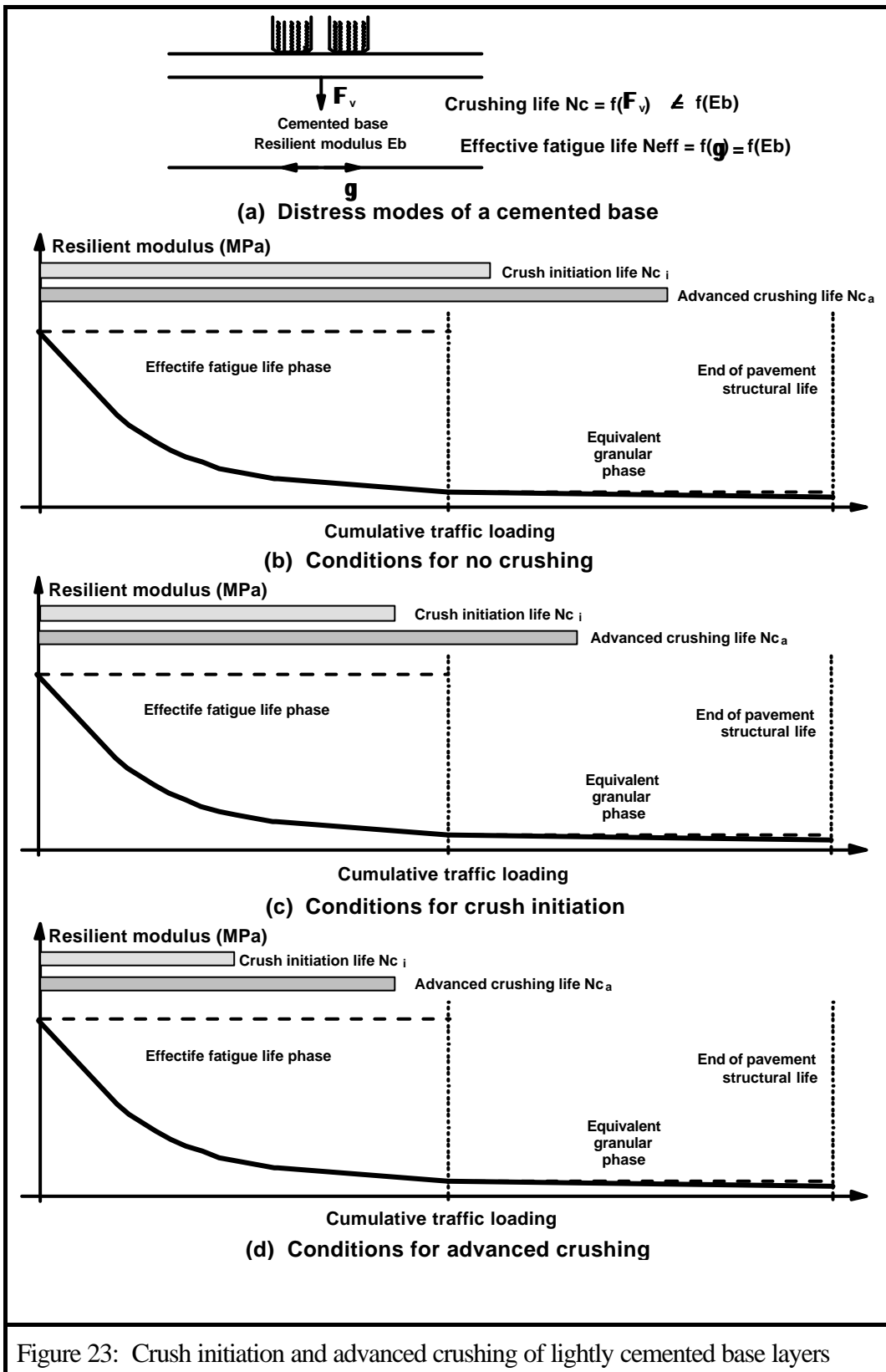
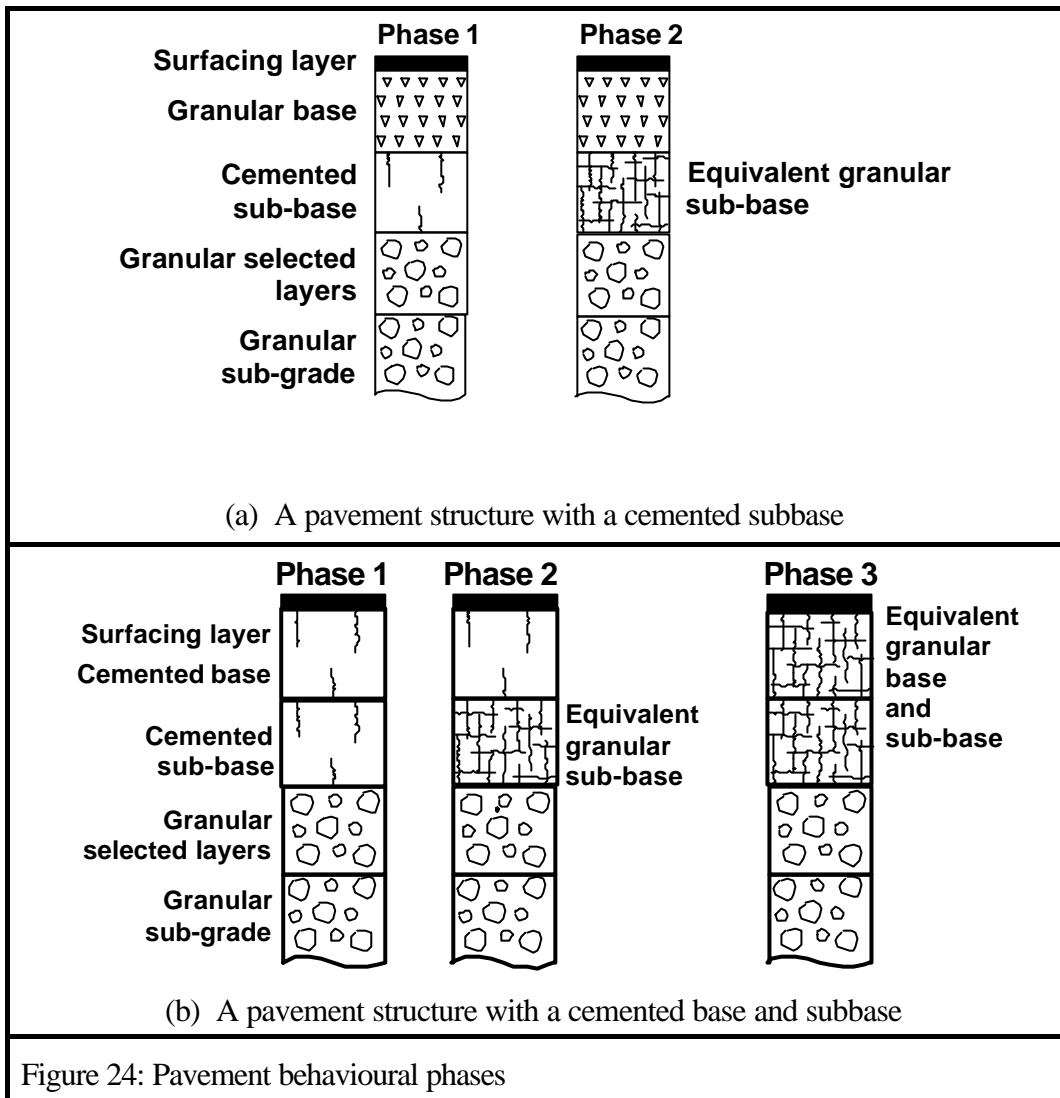


Figure 23: Crush initiation and advanced crushing of lightly cemented base layers



The process is extended along similar principles for a three phase analysis of a pavement structure incorporating two cemented layers.

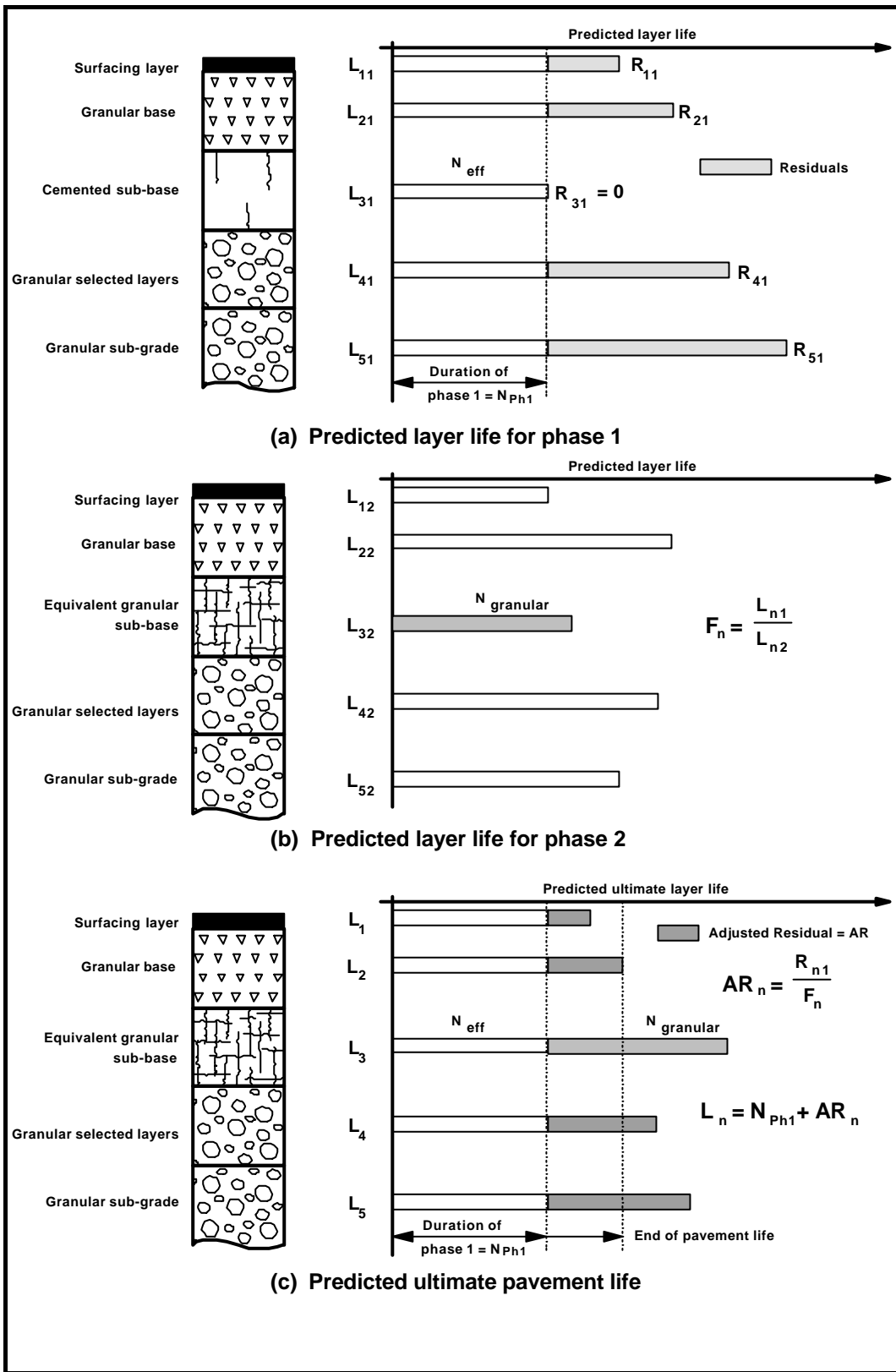


Figure 25: Calculating the ultimate pavement life for a pavement structure with cemented layers

THE PAVEMENT ANALYSIS AND DESIGN SOFTWARE (PADS) PACKAGE

A pavement analysis and design software package based on the design procedure discussed in the preceding section was written to enable the consistent application of the design procedure. This section features some of the main features of the prototype package which will soon be available commercially. The program consists of a number of pages each having a different functionality.

Data Input Pages

There are two data input pages in the program. Figure 26 shows an example of a typical opening page containing the general input, pavement geometry and material input data. The program allows material input data for a maximum of three phases depending on the number of cemented layers in the pavement system. The border of the calculate button at the top left-hand corner of the page turns red if any of the input data is changed. This alerts the user to the fact that he needs to recalculate the results. The second input page contains the load characterization data and the coordinates for a maximum of ten positions in the pavement structure at which stresses and strains are to be calculated. Figure 27 shows an example of the load characterization page.

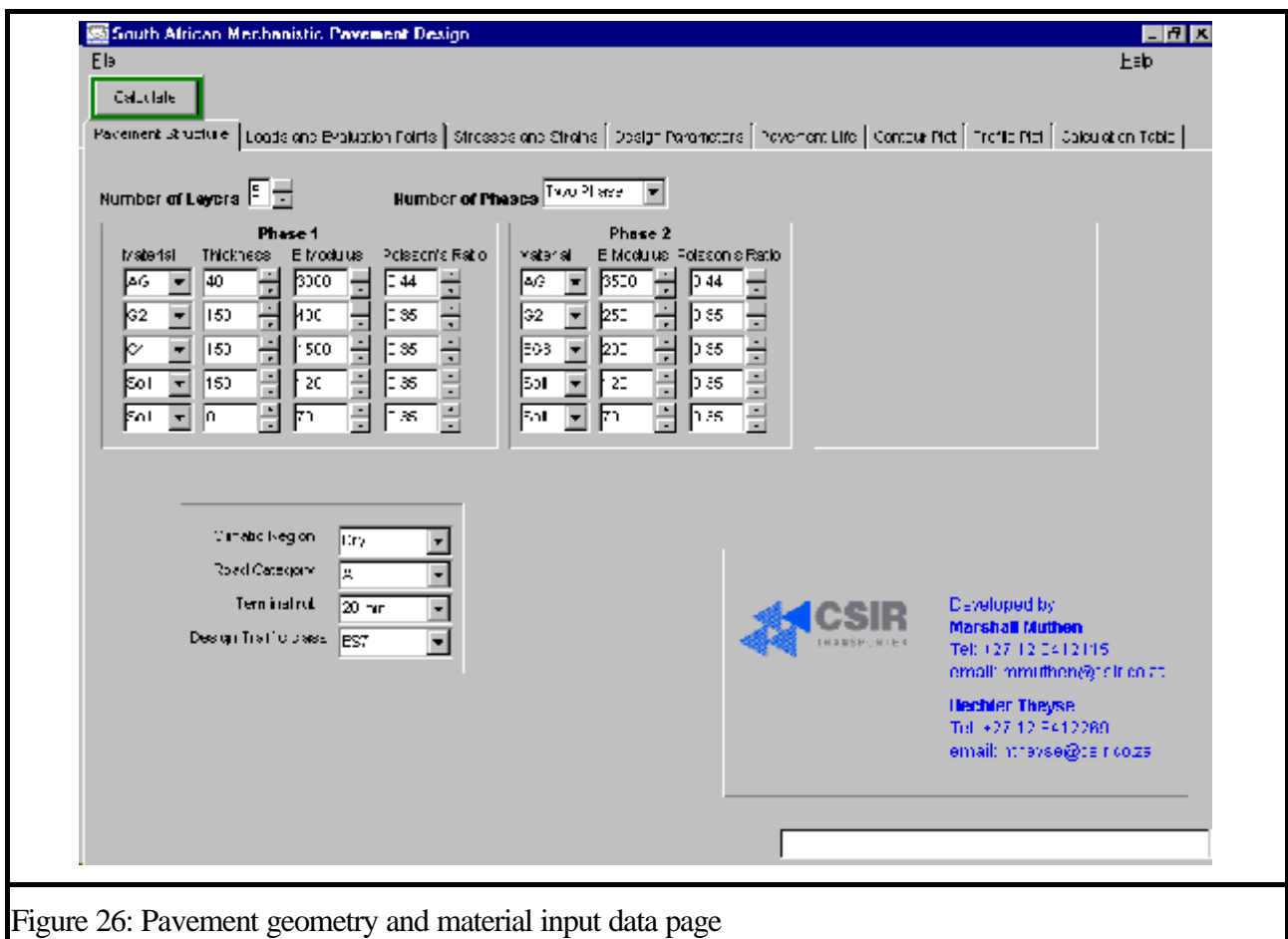


Figure 26: Pavement geometry and material input data page

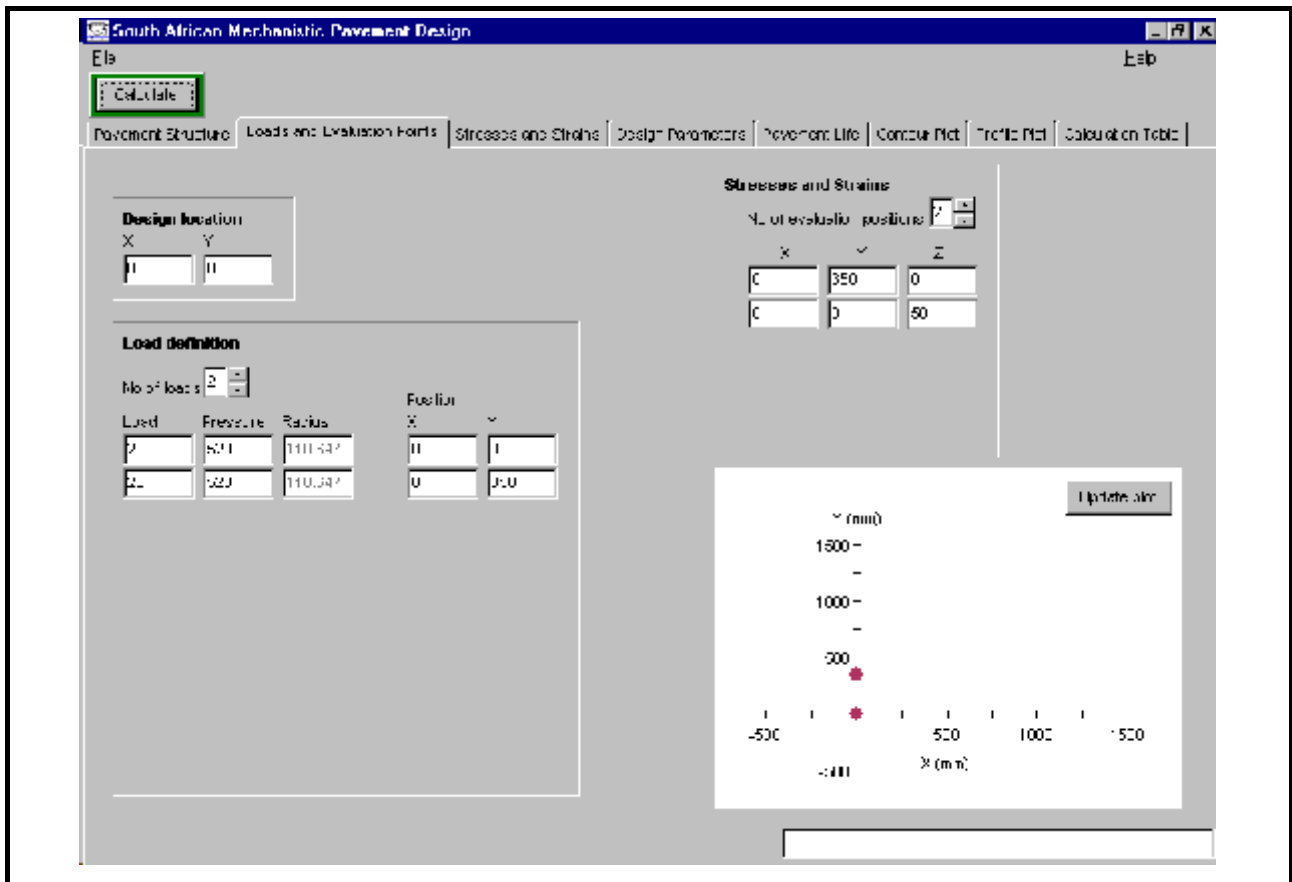


Figure 27: Load characterization and analysis location page

The design calculations are not based on the positions of the evaluation points specified on this page but are automatically determined by the program depending on the material code specified for each pavement layer. The stresses and strains at the evaluation points are reported on a separate table if the designer wants to investigate the stress condition at specific locations in the pavement structure.

Design Parameters and Pavement Life Data

The program provides a summary of the critical stress and strain parameters for each of the pavement layers depending on the material code specified for each layer for each of the analysis phases. Figure 28 shows an example of the critical parameter data which serve as input to the pavement performance models or transfer functions.

Figure 29 shows the design output from the software. The bar-chart in the top left-hand corner of the page indicates the estimated layer bearing capacity for each of the pavement layers calculated for the approximate design reliability associated with the road category specified on the pavement structure data input page. The data from which the bar-chart is drawn are shown in a table to the right of the bar-chart. In addition to the pavement bearing capacity estimate, an approximate distribution of pavement bearing capacity is shown on the graph in the bottom left-hand corner.

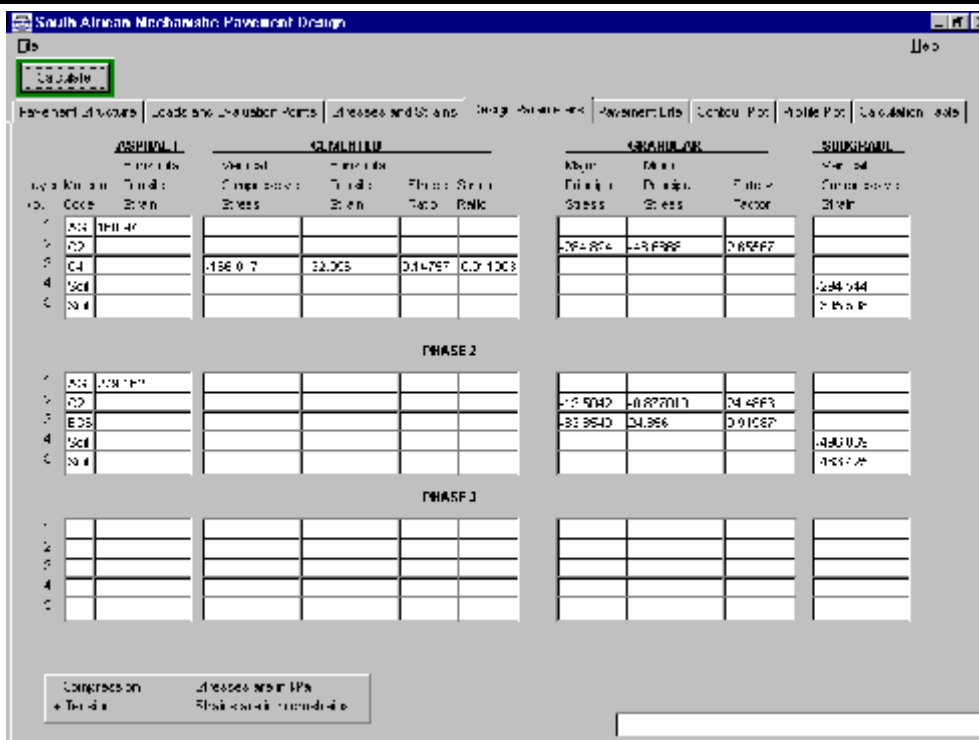


Figure 28: Summary of the critical parameters for each of the pavement layers for each of the analysis phases

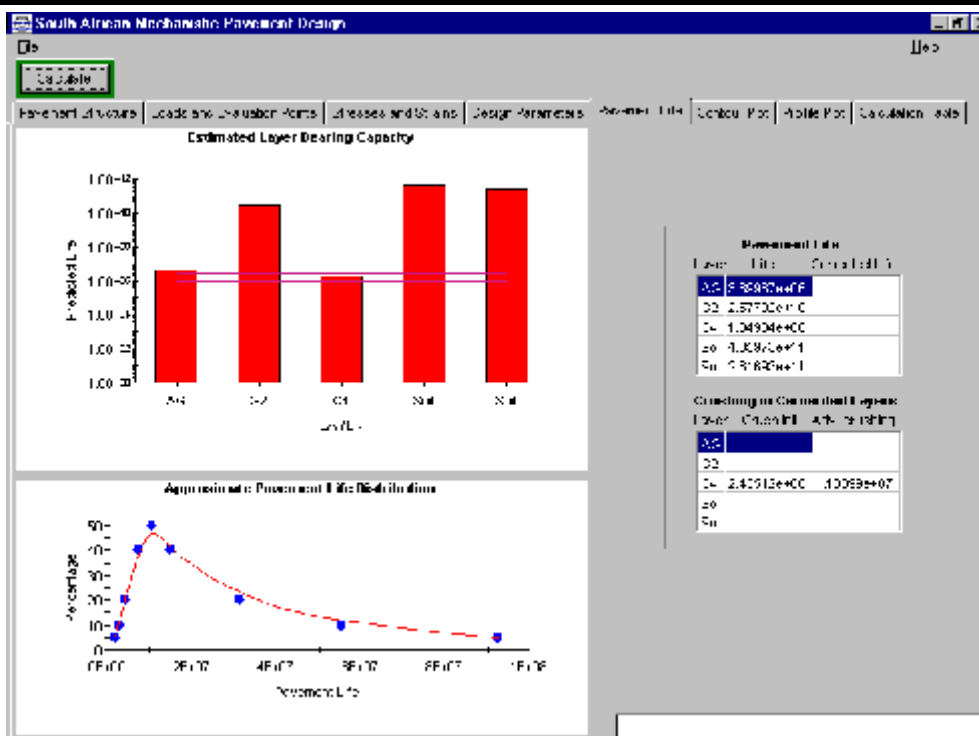


Figure 29: Design output page

Stress and Strain Analysis Output

The software also allows for a graphical representation of any of the basic stress or strain parameters. These parameters may be viewed on a profile plot or a contour plot of which examples are shown in Figures 30 and 31.

CONCLUSIONS AND RECOMMENDATIONS

The concept of approximate design reliability has been introduced in the South African Mechanistic Design Method. The pavement design catalogue of the 1996 version of the TRH4 document was revised using this updated design procedure.

This approximation of design reliability only considers the variation in the performance of a pavement for which the geometry and loading remains constant. Research on the inclusion of the effect of variation in the design input parameters is well advanced and this aspect should be the next priority for inclusion in the SAMDM.

Merely introducing probabilistic concepts in the design procedure will not necessarily increase the accuracy or precision of the design method. Continuous effort is required to increase the accuracy of the design model and to ensure that the variation predicted by the design model is in fact a true reflection of the variation in bearing capacity of real pavements.

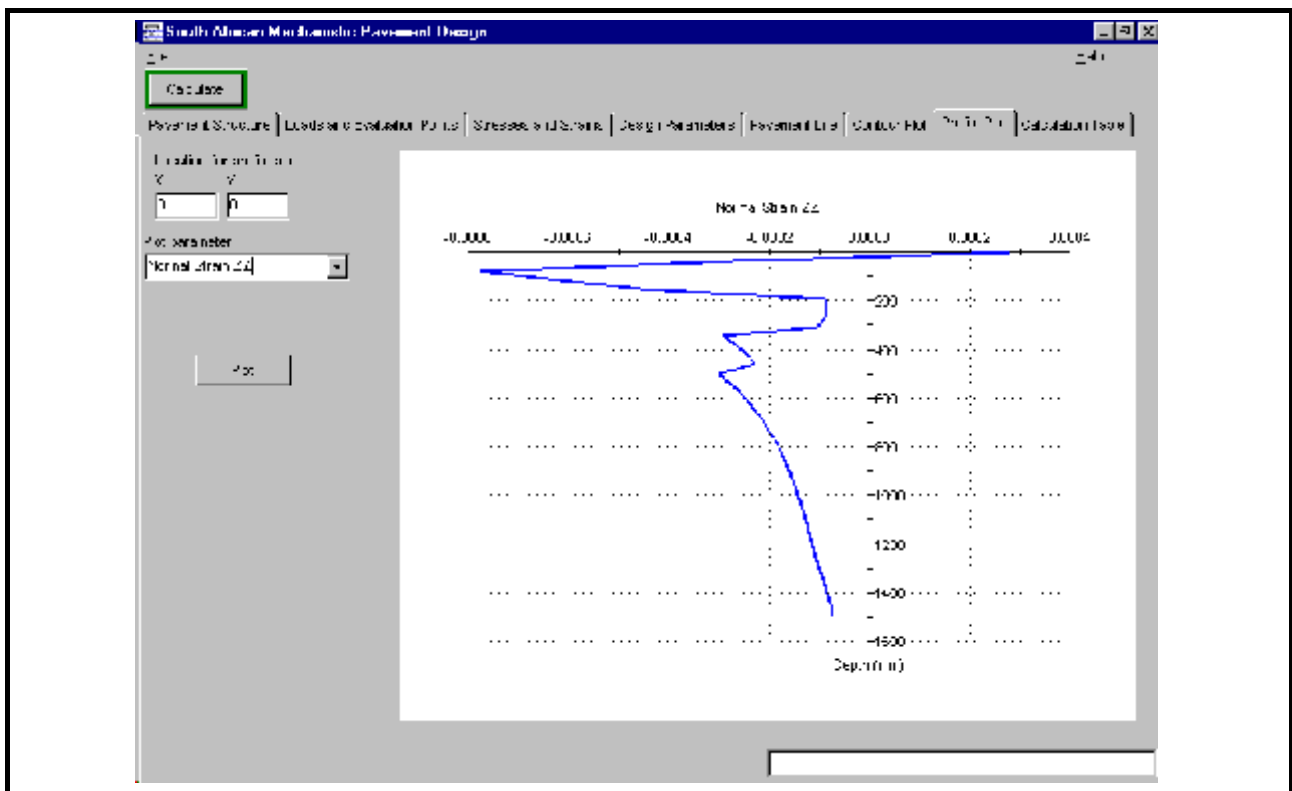


Figure 30: Example of the profile plot functionality of the PADS software

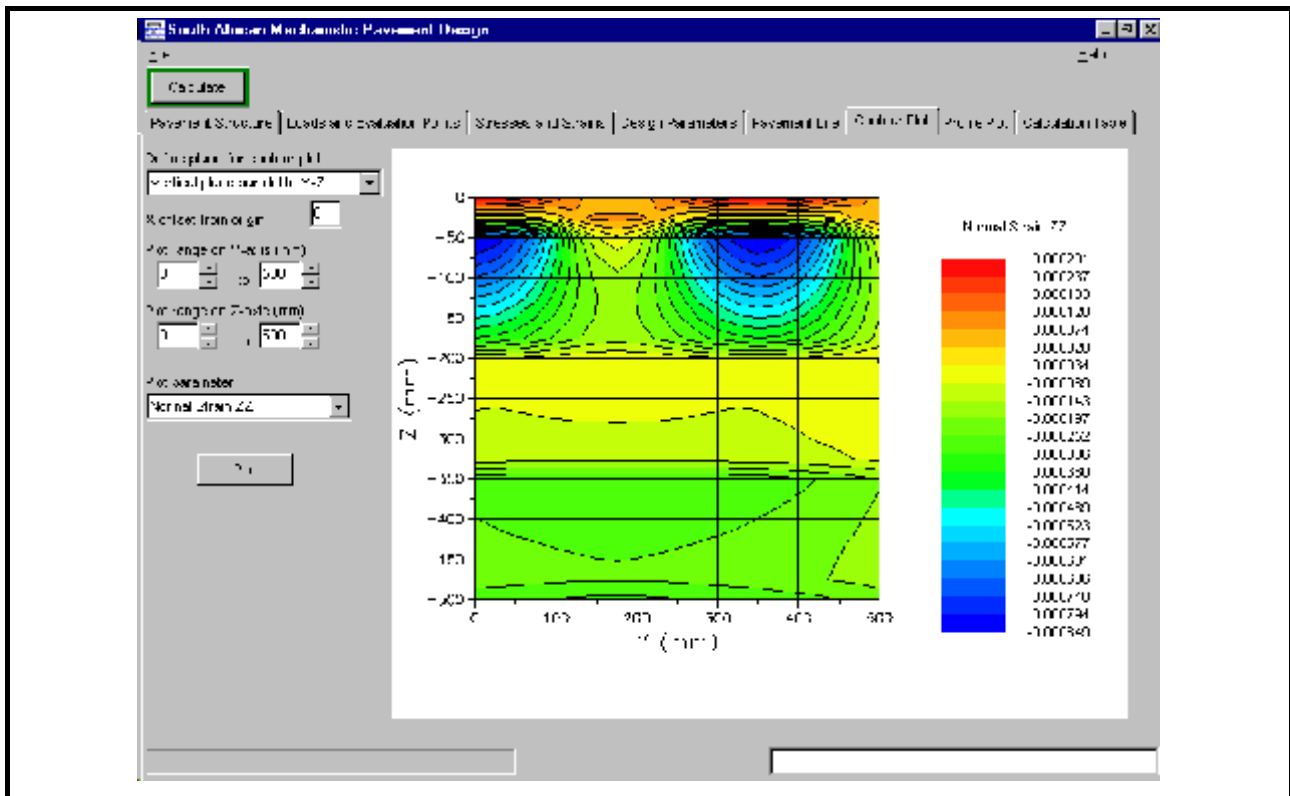


Figure 31: Example of the contour plot functionality of the PADS software

REFERENCES

1. Committee of Land Transport Officials. *Draft TRH4 (1996): Structural Design of Inter-urban and Rural Roads*. Department of Transport, Pretoria, South Africa, 1996.
2. Jooste F J. *Preprint of Paper Presented At the 7th Conference on Asphalt Pavements for Southern Africa. The influence of variability on routine pavement design*. 1999.
3. Eckmann B. *Proceedings of the 8th International Conference for Asphalt Pavements. New tools for rational pavement design*. University of Washington, Seattle, 1997.
4. Van Cauwelaert F. *Symposium on reliability-based design in civil engineering. Distributions de Rosenbleuth et fonctions corrélées*. E.P.F.L. Lausanne, Switzerland.
5. Committee of State Road Authorities. *TRH14 (1985): Guidelines for Road Construction Materials*. Department of Transport, Pretoria, South Africa, 1985.
6. Freeme C R. *Evaluation of Pavement Behaviour for Major Rehabilitation of Roads*. Technical Report RP/19/83, National Institute for Transport and Road Research, CSIR, South Africa, 1983.
7. South African Roads Board. (Jordaan G J). *Users Manual for the South African Mechanistic Pavement Rehabilitation Design Method*. Report Nr IR91/242, Department of Transport, Pretoria, South Africa, 1993.

8. South African Roads Board. (De Beer M). *The Evaluation, Analysis and Rehabilitation Design of Roads*. Report Nr IR93/296, Department of Transport, Pretoria, South Africa, 1994.
9. Shell International Petroleum Company Limited. *Shell Pavement Design Manual - Asphalt Pavements and Overlays for Road Traffic*. London, 1978.
10. Jordaan G J. *Towards Improved Procedures for the Mechanistic Analysis of Cement-treated Layers in Pavements*. Proceedings of the 7th International Conference on the Structural Design of Asphalt Pavements, Nottingham, England, 1992.
11. Heukelom W and Klomp A J G. *Dynamic Testing as a Means of Controlling Pavements During and after Construction*. Proceedings of the International Conference on the Structural Design of Asphalt Pavements, Ann Arbor, Michigan, U S A, 1962.
12. Monismith C L, Seed H B, Mitry F G and Chan C K. *Prediction of Pavement Deflections from Laboratory Tests*. Proceedings of the Second International Conference on the Structural Design of Asphalt Pavements, 1967.
13. Theyse H L, De Beer M, Prozzi J and Semmelink C J. *TRH4 Revision 1995, Phase I: Updating the Transfer Functions for the South African Mechanistic Design Method*. National Service Contract NSC24/1, Division for Roads and Transport Technology, CSIR, Pretoria, South Africa, 1995.
14. Maree J H. *Design Parameters for Crushed Stone in Pavements*. (Afrikaans) M Eng thesis, Department of Civil Engineering, Faculty of Engineering, University of Pretoria, South Africa, 1978.
15. De Beer. *Aspects of the Design and Behaviour of Road Structures Incorporating Lightly Cementitious Layers*. Ph D Thesis, Department of Civil Engineering, Faculty of Engineering, University of Pretoria, Pretoria, South Africa.